

Influence of the symmetry energy on the giant monopole resonance of neutron-rich nuclei

M. Centelles¹, S. K. Patra², X. Roca-Maza¹, B. K. Sharma³, P. D. Stevenson⁴, and X. Viñas¹

¹*Departament d'Estructura i Constituents de la Matèria and Institut de Ciències del Cosmos, Facultat de Física, Universitat de Barcelona, Diagonal 647, 08028 Barcelona, Spain*

²*Institute of Physics, Bhubaneswar 751 005, India*

³*Department of Nuclear and Atomic Physics, Tata Institute of Fundamental Research, Homi Bhabha Road, Mumbai 400 005, India*

⁴*Department of Physics, University of Surrey, Guildford, Surrey, GU2 7XH, UK*

(Dated: November 24, 2018)

Abstract

We explore the influence of the density dependence of the symmetry energy on the average excitation energy of the isoscalar giant monopole resonance (GMR) in stable and exotic neutron-rich nuclei. To this end we use the relativistic mean field model supplemented by an isoscalar-isovector meson coupling which allows precise control of the density content of the symmetry energy without compromising the success of the model for binding energies and charge radii. The range considered for the density dependence of the symmetry energy roughly covers that associated with the expected uncertainty in the measurement of the neutron radius in ²⁰⁸Pb in the upcoming PREX experiment. We obtain the average excitation energy of the GMR by applying the relativistic extended Thomas-Fermi theory in scaling and constrained calculations. These semiclassical estimates are in good agreement with the results obtained in full RPA calculations. The analysis is performed along the Pb and Zr isotopic chains. In the scaling calculations the excitation energy is larger when the symmetry energy is softer. The same happens in the constrained calculations for nuclei with small and moderate neutron excess. However, for nuclei of large isospin the constrained excitation energy becomes smaller in models having a soft symmetry energy. The effect is attributed to the presence of loosely bound outer neutrons in these isotopes. A sharp increase of the estimated width of the resonance is found in approaching the neutron drip line, even for heavy nuclei, which is enhanced when the symmetry energy is soft. In agreement with other studies, the present results suggest a sensitivity of the GMR to the properties of the symmetry energy.

PACS numbers: 24.30.Cz, 21.65.Ef, 21.60.-n, 21.30.Fe

I. INTRODUCTION

The precise determination of the nuclear equation of state (EOS) in the whole range of neutron-proton asymmetries, i.e., from nuclear to neutron matter, is one of the most fundamental problems in nuclear physics. The part of the EOS corresponding to symmetric ($N=Z$) matter is constrained by experiments involving stable nuclei which probe densities close to the nuclear matter density and small neutron-proton asymmetries. A basic property of this component of the EOS is its compression modulus K_0 , which contains the physics around the saturation density in many phenomena from nuclear structure to supernova explosions. The compression modulus K_0 is constrained in principle by the excitation energy of the isoscalar giant monopole resonance (GMR), which for medium and heavy nuclei has been accurately measured through recently improved α -particle scattering experiments [1, 2]. Theoretical calculations of the strength distribution of the GMR performed at the 1p-1h RPA level with Gogny [3], Skyrme [4, 5, 6], and relativistic mean field (RMF) interactions [7, 8] show that in order to reproduce the experimental value of the excitation energy of the GMR in ^{208}Pb (14.17 ± 0.28 MeV [1]), the compression modulus of the model in symmetric nuclear matter must lie in the range of 200–280 MeV.

The EOS of asymmetric ($N \neq Z$) matter is important not only in nuclear physics but also in astrophysics [9, 10, 11, 12, 13]. The departure of the properties of neutron-rich matter from the symmetric limit is governed by the symmetry energy. Note that to a good approximation the symmetry energy per nucleon equals the difference between the energy per particle in pure neutron matter and in symmetric matter. It is to be mentioned also that the available experimental data on ground states of nuclei, which basically correspond to systems with small and moderate values of the neutron excess $I = (N - Z)/A$, do not constrain very precisely the value of the symmetry energy at the saturation density [14, 15, 16, 17]. Rather, what seems to be better constrained by the experimental data is the symmetry energy at a density around 0.10 fm^{-3} , which corresponds to some average between the volume and surface symmetry contributions in the semi-empirical mass formula [18, 19].

A valuable connection between the properties of the EOS of isospin-rich matter and finite nuclei is provided by the neutron skin thickness of nuclei. This quantity is defined as the difference $\Delta R_{np} = R_n - R_p$ between the root-mean square (rms) radii of the neutron and proton densities of the nucleus. Some time ago Brown [14] pointed out an almost linear correlation in Skyrme forces between the value of ΔR_{np} in ^{208}Pb and the slope of the EOS of neutron matter with respect to the density at a value $\rho = 0.10 \text{ fm}^{-3}$. The same correlation has been found in the relativistic models [20, 21]. It is also known that the neutron skin thickness of ^{208}Pb in both non-relativistic and relativistic models is linearly correlated with the density derivative of the symmetry energy at $\rho = 0.10 \text{ fm}^{-3}$ [22]. Note that the neutron skins of ^{208}Pb and any other heavy neutron-rich nucleus display also a linear correlation among them [14, 23, 24].

Although the charge radius of ^{208}Pb , directly related to the rms radius of the proton density distribution, is experimentally known with extremely high accuracy ($R_{\text{ch}} = 5.5010 \pm 0.0009 \text{ fm}$ [25]), the rms radius of the neutron density of ^{208}Pb is less well known, with an experimental error often larger than 1%. This lack of accuracy in R_n in turn produces an uncertainty in the value of ΔR_{np} , which otherwise could allow a precise characterization of the density dependence of the symmetry energy at subsaturation densities. Mean field calculations with typical Skyrme or Gogny forces predict a neutron skin in ^{208}Pb around

0.1–0.2 fm. These values correspond to a slope of the symmetry energy at $\rho = 0.10 \text{ fm}^{-3}$ of 100–200 MeV fm³. However, the RMF model with successful parameter sets, as for example the celebrated NL3 model [26], usually predicts a stiffer symmetry energy, having a larger slope at $\rho = 0.10 \text{ fm}^{-3}$ (around 250 MeV fm³ in this case), and larger neutron skins of around 0.3 fm in ^{208}Pb . Though these theoretical predictions are quite different among them, all are compatible with the range of the presently accepted central values and error bars associated with R_n in ^{208}Pb . In this respect, the upcoming PREX experiment at the Jefferson Laboratory to measure the neutron rms radius of ^{208}Pb via parity-violating electron-scattering with an expected 1% accuracy [27] may be crucial to determine precisely the central value of this fundamental observable.

An accurate knowledge of the symmetry energy is essential in order to describe properly static and dynamic features of nuclei far from the naturally-occurring region of stability [28, 29, 30, 31, 32]. These exotic nuclei are produced through accelerated radioactive ion beams. From the theoretical point of view, a very efficient way to isolate and control the density dependence of the symmetry energy has been reported in Refs. [15, 16, 17]. The model consists of a standard RMF Lagrangian [33] plus an isoscalar-isovector non-linear interaction between the ω and ρ meson fields with a coupling constant Λ_V . This coupling softens the density dependence of the symmetry energy and the EOS of pure neutron matter. However, the properties of the EOS of symmetric nuclear matter (in particular the compression modulus K_0) are not affected. When the model is applied to finite nuclei, the variation of the value of the Λ_V coupling changes the neutron rms radius, but the ground-state binding energy and the proton rms radius remain practically unaltered. Thus, this additional coupling in the relativistic Lagrangian allows one to modify the size of the neutron skin thickness while preserving the agreement with the ground-state information on which the models have been calibrated.

The study of collective excitations of atomic nuclei, as for instance the GMR, near and away of the stability line is among the most interesting nuclear structure topics [5, 34, 35]. Performing measurements of the GMR in exotic nuclei is a major experimental challenge because of the low intensities and unfavorable conditions in the radioactive beams. With the advent of new experimental facilities it is hoped that measurements of the breathing mode in unstable nuclei will become possible in the future. The value of the excitation energy of the GMR is driven to a large extent by the compression modulus of symmetric nuclear matter. There is, however, a dependence on the density content of the symmetry energy in neutron-rich nuclei. For example, it is now generally acknowledged that the GMR in ^{208}Pb constrains more cleanly the incompressibility of neutron-rich matter at the neutron excess of ^{208}Pb than the incompressibility of symmetric matter [6, 36, 37, 38, 39, 40]. Thus, future experiments on the GMR in exotic nuclei might be able to furnish valuable information on the incompressibility of asymmetric matter for large isospins, and could help constrain this important piece of the nuclear EOS.

The purpose of this paper is to investigate the variation of the average excitation energy of the GMR in exotic neutron-rich nuclei of heavy and medium mass far from the stability valley, and how the uncertainty in the knowledge of the neutron rms radius in ^{208}Pb and, therefore, the density dependence of the symmetry energy, can affect the predictions of this property. To this end, we will restrict our analysis to study some estimates of the average excitation energy of the GMR that can be obtained without performing explicit RPA calculations but which carry meaningful physical information on the RPA strength. A typical example of this procedure is the so-called sum-rule approach to the RPA developed

in the non-relativistic framework using Skyrme forces [41, 42, 43] and applied to the study of the GMR in different nuclei and isotopic chains [3, 6, 41, 42, 43, 44, 45, 46]. The GMR is a collective excitation whose average properties, in general, vary smoothly with the mass number A and are rather insensitive to shell effects. Consequently, a description of these average properties of the resonance through semiclassical approaches of Thomas-Fermi type seems to be appropriate, see for example Refs. [43, 44, 47, 48]. The semiclassical relativistic extended Thomas-Fermi (RETF) theory was established in the past [49, 50, 51, 52, 53]. More recently, it has been shown that the RETF calculations of the excitation energy of the GMR, using the scaling model or performing constrained calculations, are in very good agreement with the values extracted from full relativistic RPA (RRPA) calculations [54, 55].

We will use the RMF model mentioned previously together with the RETF approach in the scaling model and in constrained calculations for describing the average excitation energies and widths of the GMR in our analysis. In the next section the basic theory is presented, in the third section the results are discussed, and the summary and conclusions are laid in the fourth section. Some details about the semiclassical RETF calculations are given in the appendices.

II. FORMALISM

A detailed description of the scaling and constrained calculations of the excitation energy of the GMR in the relativistic framework using the RETF approach has been presented elsewhere [54, 55]. Here, we shall restrict ourselves to outline the more relevant expressions, incorporating the new contributions that arise from the mixed ω - ρ meson interaction.

A. ETF energy density of the relativistic mean field model

The basic model for the present study is the relativistic mean field (RMF) theory of nucleons and mesons. As in the non-relativistic problem, the theory can be formulated in the Thomas-Fermi approach. When corrections of order \hbar^2 (in gradients of the nucleon densities and of the Dirac effective mass) to the pure Thomas-Fermi contribution are included in the energy density of the theory, it is known as the relativistic extended Thomas-Fermi (RETF) model [49, 50, 51, 52, 53].

The local energy density that we employ in the present work can be written as follows:

$$\begin{aligned} \mathcal{H} = & \mathcal{E} + W\rho + B\rho_3 + \mathcal{A}\rho_p + \frac{1}{2g_s^2} [(\nabla\Phi)^2 + m_s^2\Phi^2] + \frac{\kappa}{3!}\Phi^3 + \frac{\lambda}{4!}\Phi^4 \\ & - \frac{1}{2g_v^2} [(\nabla W)^2 + m_v^2W^2] - \frac{1}{2g_\rho^2} [(\nabla B)^2 + m_\rho^2B^2] - \Lambda_V B^2W^2 - \frac{1}{2}(\nabla\mathcal{A})^2, \quad (1) \end{aligned}$$

where $\rho = \rho_p + \rho_n$ is the baryon density, $\rho_3 = \frac{1}{2}(\rho_p - \rho_n)$ is the isovector density, and the term \mathcal{E} will be described immediately below. The energy density (1) contains scalar $\Phi = g_s\phi_0(\mathbf{r})$, vector $W = g_vV_0(\mathbf{r})$, and vector-isovector $B = g_\rho b_0(\mathbf{r})$ meson fields, as well as the Coulomb field $\mathcal{A} = eA_0(\mathbf{r})$. These fields represent, respectively, σ -meson, ω -meson, ρ -meson, and photon exchange. The cubic $\kappa\Phi^3$ and quartic $\lambda\Phi^4$ self-interactions of the scalar field are crucial to soften the equation of state of symmetric nuclear matter around the saturation point. In addition, the model is supplemented by a non-linear mixed coupling between the

ω -meson and the ρ -meson fields. This $\Lambda_V B^2 W^2$ interaction was introduced in Ref. [15] in an effort to soften the density dependence of the symmetry energy and of the neutron equation of state, which are two quantities that are predicted to be stiff by the majority of relativistic mean field models.

In the quantum approach, the contribution \mathcal{E} to the RMF energy density in Eq. (1) is given by $\mathcal{E} = \sum_{\nu} \varphi_{\nu}^{\dagger} [-i \boldsymbol{\alpha} \cdot \boldsymbol{\nabla} + \gamma_0 (m - \Phi)] \varphi_{\nu}$. Here, the φ_{ν} are single-particle Dirac wave functions, $\boldsymbol{\alpha}$ and γ_0 are the usual Dirac matrices, and m denotes the rest mass of the nucleons. The RETF representation of \mathcal{E} consists of a pure Thomas-Fermi part \mathcal{E}_0 plus a part \mathcal{E}_2 , which is of order \hbar^2 compared to \mathcal{E}_0 . The nucleon variables of the RETF energy density are the neutron and proton densities (ρ_n and ρ_p) instead of the single-particle wave functions φ_{ν} . Thereby, in the RETF approach, \mathcal{E} becomes a functional of the nucleon densities and of the Dirac effective mass $m^* = m - \Phi$. The gradient corrections contained in the \mathcal{E}_2 term provide an improved description of the nuclear surface with respect to the Thomas-Fermi treatment with only the \mathcal{E}_0 contribution. The reader can find the full RETF expression of the functional \mathcal{E} in Appendix A. We also provide there the variational Euler-Lagrange equations derived from Eq. (1) in the RETF approach for the nucleon densities and for the meson and photon fields.

The energy density \mathcal{H} is to be integrated over space to compute the total energy of the nucleus. By means of partial integrations, and on account of the variational meson field equations given in Appendix A, it is possible to write the relativistic energy density of a finite nucleus in the following form:

$$\mathcal{H} = \mathcal{E} + \frac{1}{2} \Phi \rho_s^{\text{eff}} + \frac{\kappa}{3!} \Phi^3 + \frac{\lambda}{4!} \Phi^4 + \frac{1}{2} W \rho + \frac{1}{2} B \rho_3 + \Lambda_V B^2 W^2 + \frac{1}{2} \mathcal{A} \rho_p. \quad (2)$$

Here, we have introduced the effective scalar density ρ_s^{eff} defined as

$$\rho_s^{\text{eff}} = \rho_s - \frac{\kappa}{2!} \Phi^2 - \frac{\lambda}{3!} \Phi^3. \quad (3)$$

The form given in Eq. (2) for \mathcal{H} turns out to be more practical to perform the scaling of the equations in order to compute the average excitation energy of the GMR in the scaling formalism.

B. Scaling of equations

We will use α to denote the collective coordinate of the monopole vibration. Then, a scaling transformation of the nucleon densities that preserves the normalization is

$$\rho_{q\alpha}(\mathbf{r}) = \alpha^3 \rho_q(\alpha \mathbf{r}). \quad (4)$$

Apart from the nucleon densities, the meson and Coulomb fields of the relativistic model are also modified by the scaling, owing to the fact that the variational field equations relate the fields to the densities (see the Appendices). At variance with Eq. (4), the meson fields do not scale as simple powers of α because of the finite-range character of the meson interactions. This is very clear, e.g., for the scalar field Φ , since the effective scalar density ρ_s^{eff} in the source term of the σ -meson field equation (see Eq. (A5) in Appendix A) transforms not only due to the scaling of ρ_q but also of the Φ field itself. To deal with this, it is convenient to write the scaled Dirac effective mass $m_{\alpha}^*(\mathbf{r}) = m - \Phi_{\alpha}(\mathbf{r})$ in the form [54, 55]

$$m_{\alpha}^*(\mathbf{r}) \equiv \alpha \tilde{m}^*(\alpha \mathbf{r}). \quad (5)$$

The quantity \tilde{m}^* carries an implicit dependence on α besides its parametric dependence on $\alpha\mathbf{r}$. With Eqs. (4) and (5), the energy density \mathcal{E} and the scalar density ρ_s of the RETF model can be shown to scale with α , respectively, as $\mathcal{E}_\alpha(\mathbf{r}) = \alpha^4 \mathcal{E}[\rho_q(\alpha\mathbf{r}), \tilde{m}^*(\alpha\mathbf{r})] \equiv \alpha^4 \tilde{\mathcal{E}}(\alpha\mathbf{r})$ and as $\rho_{s\alpha}(\mathbf{r}) = \alpha^3 \rho_s[\rho_q(\alpha\mathbf{r}), \tilde{m}^*(\alpha\mathbf{r})] \equiv \alpha^3 \tilde{\rho}_s(\alpha\mathbf{r})$ [54, 55]. The tilded quantities $\tilde{\mathcal{E}}$ and $\tilde{\rho}_s$ have the same expression as \mathcal{E} and ρ_s given in Appendix A if m^* is replaced by \tilde{m}^* . Taking into account the above considerations, the scaled form of the energy density of the present model becomes

$$\begin{aligned} \mathcal{H}_\alpha = \alpha^3 & \left[\alpha \tilde{\mathcal{E}} + \frac{1}{2} \Phi_\alpha \tilde{\rho}_s^{\text{eff}} + \frac{1}{3!} \frac{\kappa}{\alpha^3} \Phi_\alpha^3 + \frac{1}{4!} \frac{\lambda}{\alpha^3} \Phi_\alpha^4 \right. \\ & \left. + \frac{1}{2} W_\alpha \rho + \frac{1}{2} B_\alpha \rho_3 + \frac{\Lambda_V}{\alpha^3} B_\alpha^2 W_\alpha^2 + \frac{1}{2} \mathcal{A}_\alpha \rho_p \right], \end{aligned} \quad (6)$$

with the definition $\tilde{\rho}_s^{\text{eff}} = \tilde{\rho}_s - \kappa \Phi_\alpha^2 / 2\alpha^3 - \lambda \Phi_\alpha^3 / 2\alpha^3$.

The calculation of the first derivative of the scaled energy $E(\alpha) = \int d\mathbf{r} \mathcal{H}_\alpha$ with respect to the collective coordinate α gives

$$\begin{aligned} & \frac{\partial}{\partial \alpha} \int d(\alpha\mathbf{r}) \frac{\mathcal{H}_\alpha(\mathbf{r})}{\alpha^3} \\ &= \int d(\alpha\mathbf{r}) \left[\tilde{\mathcal{E}} - \tilde{m}^* \tilde{\rho}_s - \frac{1}{2} \tilde{\rho}_s^{\text{eff}} \frac{\partial \Phi_\alpha}{\partial \alpha} + \frac{1}{2} \Phi_\alpha \frac{\partial \tilde{\rho}_s^{\text{eff}}}{\partial \alpha} - \frac{\kappa}{2\alpha^4} \Phi_\alpha^3 - \frac{\lambda}{8\alpha^4} \Phi_\alpha^4 - \frac{3\Lambda_V}{\alpha^4} B_\alpha^2 W_\alpha^2 \right. \\ & \quad \left. + \frac{1}{2} \rho \frac{\partial W_\alpha}{\partial \alpha} + \frac{1}{2} \rho_3 \frac{\partial B_\alpha}{\partial \alpha} + \frac{2\Lambda_V}{\alpha^3} \left(B_\alpha W_\alpha^2 \frac{\partial B_\alpha}{\partial \alpha} + B_\alpha^2 W_\alpha \frac{\partial W_\alpha}{\partial \alpha} \right) + \frac{1}{2} \rho_p \frac{\partial \mathcal{A}_\alpha}{\partial \alpha} \right], \end{aligned} \quad (7)$$

where we have used that $\partial \tilde{\mathcal{E}} / \partial \alpha = \tilde{\rho}_s \partial \tilde{m}^* / \partial \alpha$ (due to the fact that $\tilde{\rho}_s = \delta \tilde{\mathcal{E}} / \delta \tilde{m}^*$) together with the result $\partial \tilde{m}^* / \partial \alpha = -\alpha^{-1} (\tilde{m}^* + \partial \Phi_\alpha / \partial \alpha)$ [because $\partial m_\alpha^* / \partial \alpha = \tilde{m}^* + \alpha \partial \tilde{m}^* / \partial \alpha = -\partial \Phi_\alpha / \partial \alpha$, following from the definition of \tilde{m}^* in Eq. (5)]. The derivatives of the fields with respect to the scaling parameter α can be removed from expression (7) with the help of the field equations satisfied by the scaled meson and photon fields, as we describe in Appendix B. Finally, Eq. (7) reads

$$\begin{aligned} & \frac{\partial}{\partial \alpha} \int d(\alpha\mathbf{r}) \frac{\mathcal{H}_\alpha(\mathbf{r})}{\alpha^3} \\ &= \int d(\alpha\mathbf{r}) \left[\tilde{\mathcal{E}} - \tilde{m}^* \tilde{\rho}_s - \frac{1}{2} \tilde{\rho}_s^{\text{eff}} \Phi_\alpha \frac{m_s^2}{g_s^2} \frac{\Phi_\alpha^2}{\alpha^4} - \frac{\kappa}{2\alpha^4} \Phi_\alpha^3 - \frac{\lambda}{8\alpha^4} \Phi_\alpha^4 \right. \\ & \quad \left. + \frac{1}{2\alpha} \rho W_\alpha + \frac{m_v^2}{g_v^2} \frac{W_\alpha^2}{\alpha^4} + \frac{1}{2\alpha} \rho_3 B_\alpha + \frac{m_\rho^2}{g_\rho^2} \frac{B_\alpha^2}{\alpha^4} + \frac{\Lambda_V}{\alpha^4} B_\alpha^2 W_\alpha^2 + \frac{1}{2\alpha} \mathcal{A}_\alpha \rho_p \right]. \end{aligned} \quad (8)$$

The stationarity condition of the energy against scaling implies that Eq. (8) must vanish at $\alpha = 1$, which leads to the virial theorem for the present model. It can be used to rewrite the expression of the ground-state energy of the relativistic model, with the following (somewhat surprising!) result:

$$E = \int d\mathbf{r} \mathcal{H} = \int d\mathbf{r} \left[m \rho_s + \frac{m_s^2}{g_s^2} \Phi^2 - \frac{m_v^2}{g_v^2} W^2 - \frac{m_\rho^2}{g_\rho^2} B^2 + \frac{\kappa}{3!} \Phi^3 \right], \quad (9)$$

where all of the nucleonic contributions are summarized in the scalar density ρ_s , and where the massless photon field and the quartic couplings such as $\lambda\Phi^4$ and $\Lambda_V B^2 W^2$ do not provide explicit contributions.

C. Energy of the GMR in the scaling approach

It is customary to write the excitation energy of the isoscalar giant monopole resonance of a finite nucleus of mass number A as

$$E_M = \sqrt{\frac{AK_A}{B_M}}, \quad (10)$$

where K_A is called the compression modulus or incompressibility of the finite nucleus and B_M is called the mass or inertia parameter of the monopole oscillation. In the scaling approach, the value of K_A is obtained from the restoring force of the monopole vibration. Differentiating Eq. (8) again with respect to the scaling parameter α and then setting $\alpha = 1$, one arrives at the result

$$\begin{aligned} K_A^{\text{scal}} &= \frac{1}{A} \left[\frac{\partial^2}{\partial \alpha^2} \int d(\alpha \mathbf{r}) \frac{\mathcal{H}_\alpha(\mathbf{r})}{\alpha^3} \right]_{\alpha=1} \\ &= \frac{1}{A} \int d\mathbf{r} \left[3 \left(\frac{m_s^2}{g_s^2} \Phi^2 - \frac{m_v^2}{g_v^2} W^2 - \frac{m_\rho^2}{g_\rho^2} B^2 + \frac{\kappa}{3!} \Phi^3 \right) - m \frac{\partial \tilde{\rho}_s}{\partial \alpha} \right. \\ &\quad \left. - \left(2 \frac{m_s^2}{g_s^2} \Phi + \frac{\kappa}{2} \Phi^2 \right) \frac{\partial \Phi_\alpha}{\partial \alpha} + 2 \frac{m_v^2}{g_v^2} W \frac{\partial W_\alpha}{\partial \alpha} + 2 \frac{m_\rho^2}{g_\rho^2} B \frac{\partial B_\alpha}{\partial \alpha} \right]_{\alpha=1}, \end{aligned} \quad (11)$$

where we have $(\partial \tilde{\rho}_s / \partial \alpha)_{\alpha=1} = -(\partial \rho_s / \partial m^*) (m^* + (\partial \Phi_\alpha / \partial \alpha)_{\alpha=1})$. The expression (11) depends on the meson fields and on their derivatives with respect to the scaling parameter α evaluated at equilibrium. These derivatives can be computed by differentiation of the corresponding scaled meson field equations with respect to α , and by solving them at $\alpha = 1$, as we describe in Appendix B (also see Ref. [55]). We will use the notation E_M^{scal} to refer to the excitation energy of the GMR calculated in the scaling approach, namely,

$$E_M^{\text{scal}} = \sqrt{\frac{AK_A^{\text{scal}}}{B_M}}. \quad (12)$$

The mass parameter of the monopole resonance is given by the expression [55, 56, 57]

$$B_M = \int d\mathbf{r} r^2 \mathcal{H}. \quad (13)$$

We note that in the non-relativistic limit it reads

$$B_M^{\text{nr}} = \int d\mathbf{r} r^2 m \rho = m A \langle r^2 \rangle, \quad (14)$$

where m is the nucleon rest mass. Because of the large contribution of the nucleon rest mass term $m\rho$ to \mathcal{H} in the integrand of B_M in Eq. (13), the value of the excitation energy of the resonance is little modified by using either B_M or B_M^{nr} in the calculations.

D. Energy of the GMR in the constrained approach

One also can study the average excitation energy of the giant monopole resonance through constrained calculations [41, 55, 58, 59, 60, 61]. For that purpose, one solves the problem associated with the constrained functional

$$\int d\mathbf{r}[\mathcal{H} - \eta r^2 \rho] = E(\eta) - \eta \int d\mathbf{r} r^2 \rho. \quad (15)$$

The densities, fields, and energy obtained from the solution of the variational equations deduced from Eq. (15) depend on the value of the parameter η at which one performs the calculation. By expanding $E(\eta)$ in a harmonic approximation about its minimum, located at the ground-state rms radius R_0 (corresponding to $\eta = 0$), one obtains the compression modulus of the finite nucleus in the constrained approach:

$$K_A^{\text{cons}} = \frac{1}{A} R_0^2 \left(\frac{\partial^2 E(\eta)}{\partial R_\eta^2} \right)_{\eta=0}. \quad (16)$$

Here, $R_\eta^2 = \langle r^2 \rangle_\eta$ is the square mass radius of the nucleus computed with the density ρ of Eq. (15). One can show that Eq. (16) can be rewritten in the following equivalent forms:

$$K_A^{\text{cons}} = -4R_0^4 \left(\frac{\partial R_\eta^2}{\partial \eta} \right)_{\eta=0}^{-1} = 4AR_0^4 \left(\frac{\partial^2 E(\eta)}{\partial \eta^2} \right)_{\eta=0}^{-1}, \quad (17)$$

which subsidiarily provide a practical means to check the accuracy of the performed numerical calculations. Finally, the excitation energy of the constrained isoscalar monopole vibration is computed as

$$E_M^{\text{cons}} = \sqrt{\frac{AK_A^{\text{cons}}}{B_M}}. \quad (18)$$

E. Expressions in the non-relativistic sum-rule approach

In the non-relativistic RPA theory, the scaling and constrained energies of the isoscalar giant monopole resonance can be written in terms of ratios of integral moments $m_k = \int_0^\infty d\omega \omega^k S(\omega)$ of the strength function $S(\omega)$ [41, 42, 43]:

$$E_M^{\text{scal}} = E_3 \equiv \sqrt{\frac{m_3}{m_1}}, \quad E_M^{\text{cons}} = E_1 \equiv \sqrt{\frac{m_1}{m_{-1}}}. \quad (19)$$

This is due to the fact that in the non-relativistic theory some moments m_k can be computed from RPA sum-rule expressions, as an alternative option to evaluate the m_k directly from $S(\omega)$ [41, 42, 43]. In this way it is proven that the cubic energy-weighted moment m_3 is equivalent to the second derivative of the scaled energy, and that the energy-weighted moment m_1 and the inverse energy-weighted moment m_{-1} are equivalent, respectively, to the following results:

$$m_1 = \frac{2}{m} A \langle r^2 \rangle, \quad \text{i.e., } m_1 = \frac{2}{m^2} B_M^{\text{nr}}, \quad (20)$$

and

$$m_{-1} = -\frac{1}{2}A \left(\frac{\partial R_\eta^2}{\partial \eta} \right)_{\eta=0}. \quad (21)$$

The integral moments of the non-relativistic RPA strength function are known to obey certain inequalities and, in particular, one can derive the useful condition

$$E_1 \leq E_x = \frac{m_1}{m_0} \leq E_3, \quad (22)$$

where E_x is the centroid energy of the GMR evaluated from the ratio of the m_1 moment to the m_0 moment. It can be shown [41] that an upper bound for the width, or variance, of the giant monopole resonance is provided by the quantity

$$\sigma = \frac{1}{2} \sqrt{E_3^2 - E_1^2}. \quad (23)$$

The calculations carried out for stable nuclei show that E_3 and E_1 become increasingly close with increasing nuclear mass. Therefore, in heavy nuclei the value of the width σ decreases and the monopole strength becomes more concentrated around a single peak [41], which is the situation found in experiment. Note that the RPA theory accounts properly for the escape width of the resonance. However, it cannot account for the spreading component of the width, which is related to more complex configurations than those included in the RPA calculations. As a consequence, the resonance width estimated by Eq. (23) can be lower than the experimentally measured value [43].

In terms of the moments of the strength function, in the non-relativistic RPA theory the compression modulus of the finite nucleus takes the form $K_A^{\text{scal}} = (m^2/2A) m_3$ in the scaling approach and $K_A^{\text{cons}} = (m^2/2A) m_1^2/m_{-1}$ in the constrained approach [41]. These expressions, together with Eqs. (19)–(21), suggest an appealing analogy between Eqs. (12) and (18) given previously for the GMR energy in the relativistic model and the non-relativistic formalism of sum rules. However, to our knowledge, the sum-rule approach is not derived in the relativistic RPA (RRPA) theory.

III. RESULTS AND DISCUSSIONS

A. Comparison of relativistic ETF and Hartree-RPA results

First, in this section we test with some examples the relativistic extended Thomas-Fermi (RETF) approach to ground-state properties and to the GMR vis-à-vis Hartree and relativistic RPA calculations. To this end, we report in Table I semiclassical RETF results for the binding energy, neutron skin thickness, and excitation energy of the GMR in the stable nuclei ^{208}Pb and ^{90}Zr . Our results have been computed with the NL3 mean field interaction [26] supplemented by the nonlinear Λ_V coupling between the ω -meson and ρ -meson fields [15]. The modification of the value of Λ_V allows one to investigate the change of the results with varying the density dependence of the symmetry energy. We compare our RETF calculations with the corresponding Hartree and relativistic RPA values. We have taken the RPA excitation energies of the GMR reported in Table I from Ref. [39].

For the coupling constant Λ_V we use the values 0.00, 0.01, 0.02, and 0.03 (models denoted as NL3.00, NL3.01, NL3.02, and NL3.03). It is known that the binding energy of nuclei

TABLE I: Relativistic Hartree-RPA and relativistic extended Thomas-Fermi values obtained with the NL3 model plus the isoscalar-isovector coupling Λ_V for the binding energy per particle (MeV), neutron skin thickness $\Delta R_{np} = R_n - R_p$ (fm), and excitation energy of the GMR (MeV) in ^{208}Pb and ^{90}Zr . The GMR centroid energies m_1/m_0 are from Ref. [39].

^{208}Pb :							
Model	Hartree-RPA			RETF			
	B/A	ΔR_{np}	m_1/m_0	B/A	ΔR_{np}	E_M^{cons}	E_M^{scal}
NL3.00	7.87	0.28	14.32	7.99	0.23	13.92	14.58
NL3.01	7.89	0.25	14.43	8.01	0.20	13.97	14.61
NL3.02	7.91	0.22	14.57	8.02	0.17	14.07	14.70
NL3.03	7.91	0.20	14.74	8.03	0.15	14.20	14.83
^{90}Zr :							
Model	Hartree-RPA			RETF			
	B/A	ΔR_{np}	m_1/m_0	B/A	ΔR_{np}	E_M^{cons}	E_M^{scal}
NL3.00	8.69	0.11	18.62	8.91	0.10	19.04	19.53
NL3.01	8.69	0.10	18.67	8.91	0.09	19.05	19.54
NL3.02	8.70	0.09	18.69	8.92	0.08	19.08	19.58
NL3.03	8.70	0.08	18.75	8.92	0.07	19.12	19.62

constrains an average of the symmetry energy at saturation density and the surface symmetry energy, rather than the individual value of the symmetry energy at saturation [15, 16, 17, 18, 19]. Thus, as done in earlier literature [15, 16, 17, 23, 24], we constrain the symmetry energy $S(\rho)$ of the models to take a value of 25.67 MeV at a Fermi momentum $k_F = 1.15 \text{ fm}^{-1}$ (i.e., at a subsaturation density $\rho \approx 0.10 \text{ fm}^{-3}$). This implies that the coupling constant g_ρ of the NL3 interaction has to be suitably adjusted for each value of the isoscalar-isovector Λ_V coupling. As a consequence, the value $S(\rho_0)$ of the symmetry energy at the saturation density ρ_0 changes with the Λ_V parameter. We find the results $S(\rho_0) = 37.4, 35.0, 33.2$, and 31.7 MeV when we vary Λ_V from 0.00 to 0.03. That is, the symmetry energy $S(\rho)$ of the model around saturation becomes softer (it increases more slowly with the nuclear density) when the value of the Λ_V parameter is larger. Further details on the behavior of $S(\rho)$ in the NL3 model supplemented by the Λ_V coupling can be found in Ref. [23]. In Table I, one sees that the neutron skin thickness of a neutron-rich nucleus is significantly reduced by increasing the value of the Λ_V coupling, i.e., the models with a softer symmetry energy give rise to smaller neutron skins.

From Table I we observe that in the semiclassical RETF approach the binding energies are larger, and the neutron skins smaller, than in the corresponding quantal Hartree calculations. However, one has to note the fact that, when the Λ_V coupling is changed from 0.00 to 0.03, in both the Hartree and RETF calculations the binding energies remain similarly constant and the neutron skins decrease by practically the same amount of 0.08 fm in ^{208}Pb and of 0.03 fm in ^{90}Zr . Therefore, the RETF approach predicts the same variation of the results with Λ_V as the quantal Hartree calculations do. This implies that the rate of change of the results with the density dependence of the symmetry energy in the present model is well described by the RETF method. As a further test, which is motivated also because later we will study RETF results along isotopic chains, in Fig. 1 we plot for Pb isotopes the difference

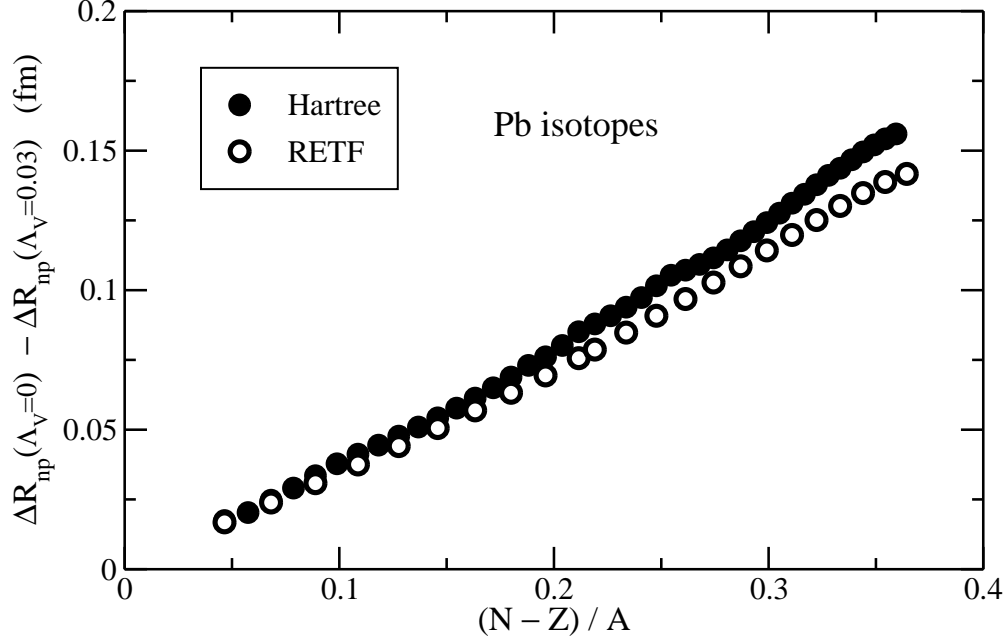


FIG. 1: Difference between the values of the neutron skin thickness ΔR_{np} obtained with $\Lambda_V = 0$ and with $\Lambda_V = 0.03$ for lead isotopes. The results of the RETF method are compared with the results of quantal Hartree calculations.

between the value of the neutron skin thickness of the nucleus calculated with $\Lambda_V = 0.00$ and with $\Lambda_V = 0.03$. We observe by comparison with the corresponding quantal Hartree results, that the RETF approach performs rather satisfactorily along the Pb isotopic chain in predicting the size of the modification of the neutron skin thickness induced by the change of the density dependence of the symmetry energy of the model.

With regard to the average excitation energies of the GMR, Table I shows the scaled and constrained values (i.e., E_M^{scal} of Section IIC and E_M^{cons} of Section IID) for ^{208}Pb and ^{90}Zr calculated in the RETF approach. We compare our RETF results with the values of the centroid energy m_1/m_0 of the GMR extracted from the RRPA strength, which have been reported in Ref. [39]. We see that for the ^{208}Pb nucleus, the RRPA centroid energies nicely lie in between the RETF scaled and constrained estimates, as it is required in the non-relativistic sum-rule approach to the RPA [41, 42, 43] [see Eq. (22)]. In the case of the ^{90}Zr nucleus, the RETF estimates are slightly larger than the RRPA average energies. Nevertheless, as it happens in the case of ^{208}Pb , the semiclassical average excitation energies as a function of Λ_V display the tendency of the RRPA excitation energies. In summary, the RETF approach appears as a reasonable starting point to discuss the influence of the density dependence of the symmetry energy on the GMR of neutron-rich nuclei.

B. GMR in heavy neutron-rich nuclei

In the present section we analyze the predictions obtained with the RETF method for neutron-rich nuclei of heavy mass. Specifically, we discuss the results calculated for the drip line nucleus ^{266}Pb (that has a neutron-proton asymmetry parameter $I = (N-Z)/A = 0.383$) in comparison with the results derived for the stable isotope ^{208}Pb (that has $I = 0.212$). For

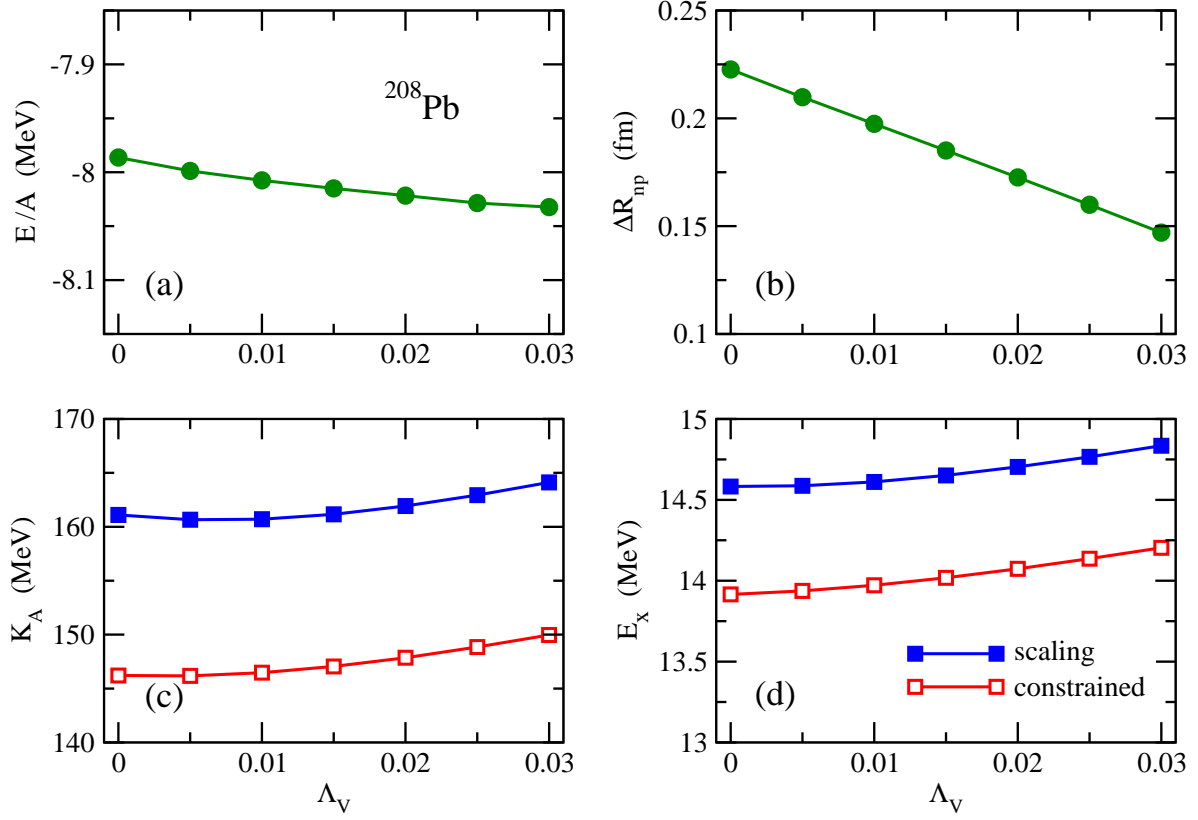


FIG. 2: (Color online) Dependence with the value of the isoscalar-isovector coupling Λ_V of the energy per particle (a), neutron skin thickness (b), finite nucleus compression modulus (c), and average excitation energy of the GMR (d) for the ^{208}Pb nucleus.

this purpose, we display as a function of the coupling constant Λ_V , in Fig. 2 for ^{208}Pb and in Fig. 3 for ^{266}Pb , the calculated values of the energy per particle, the neutron skin thickness, the compression modulus of the finite nucleus, and the average excitation energy of the GMR obtained in the scaling and constrained approaches. We recall that the coupling Λ_V induces a change of the density dependence of the symmetry energy in the relativistic mean field model. The characterization of the density dependence of the symmetry energy is instrumental to our knowledge of the equation of state of neutron-rich matter [62]. Unfortunately, to date it is not sufficiently well constrained by the available data and observations. There exists a considerable recent effort in the community oriented at better understanding the density content of the symmetry energy in the regime of subsaturation densities, relevant for finite nuclei, from the phenomenology of intermediate-energy heavy ion reactions, nuclear collective excitations, and ground-state properties of nuclei, see for example Refs. [2, 19, 62, 63, 64, 65, 66, 67, 68, 69].

As we have mentioned, the RMF Lagrangian supplemented by the non-linear interaction between the ω and ρ meson fields leaves the binding energy of the nucleus almost independent of the strength of the coupling constant Λ_V , at least for moderate values of this coupling. We note that this fact happens not only in the case of stable nuclei, which we have seen previously in Table I for ^{208}Pb and ^{90}Zr , but also in the case of a very neutron-rich nucleus such as ^{266}Pb , as we can realize from Fig. 3. We observe that for both lead isotopes, ^{208}Pb and ^{266}Pb , the neutron thickness decreases almost linearly with an increase of Λ_V . The

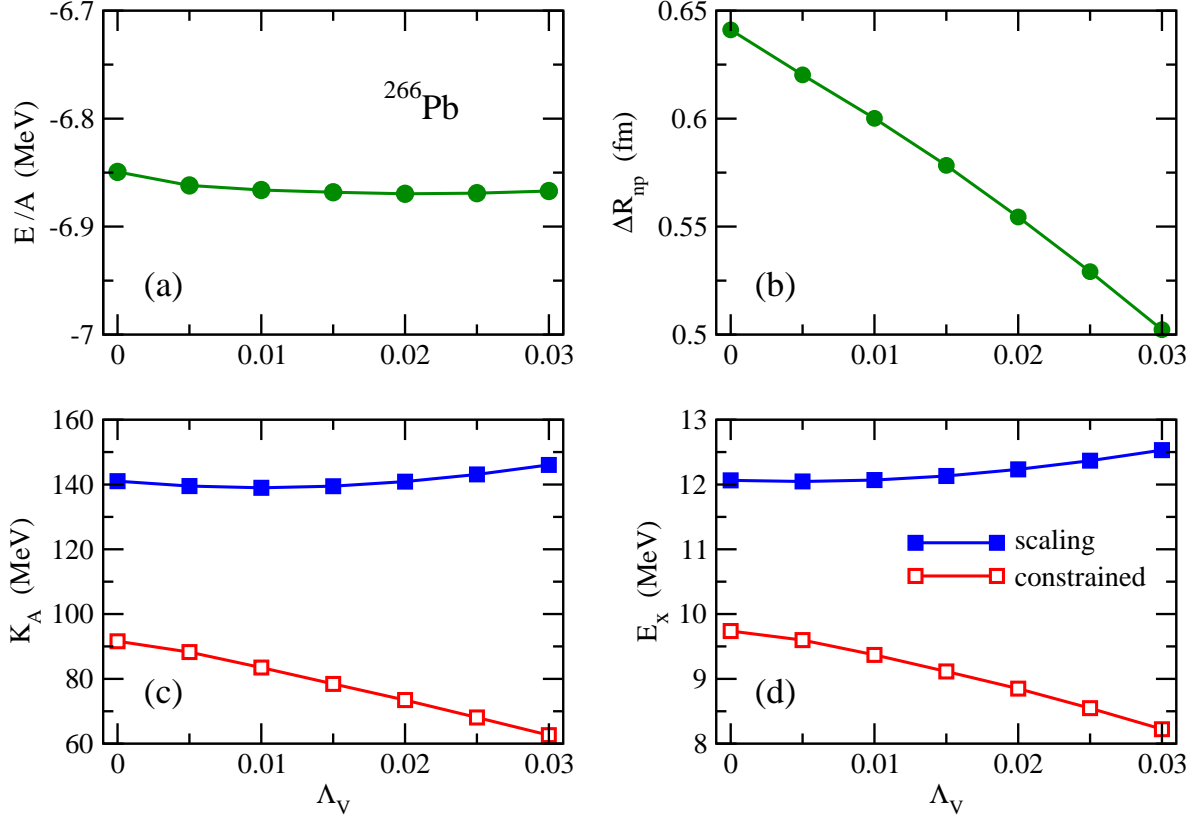


FIG. 3: (Color online) Dependence with the value of the isoscalar-isovector coupling Λ_V of the energy per particle (a), neutron skin thickness (b), finite nucleus compression modulus (c), and average excitation energy of the GMR (d) for the ^{266}Pb nucleus.

reduction is about 0.08 fm for ^{208}Pb and 0.15 fm for ^{266}Pb when Λ_V changes from 0.00 to 0.03. These variations correspond, respectively, to $\sim 30\%$ and $\sim 25\%$ of the values found at $\Lambda_V = 0.00$. It is worth mentioning that the alluded variation of the neutron skin thickness of ^{208}Pb is close to the uncertainty of this magnitude associated to a 1% error in the neutron rms radius, which is the expected accuracy to be achieved in the measurement of R_n of ^{208}Pb in the commissioned PREX experiment [27]. The rms radius R_p of the proton density distribution of ^{208}Pb and ^{266}Pb remains nearly constant when the value of the Λ_V coupling varies, and therefore we do not display the calculated R_p values in Figs. 2 and 3.

The average excitation energy of the GMR calculated in the RETF approach involves the knowledge of the finite nucleus compression modulus K_A , or restoring force of the resonance. We display K_A in Figs. 2(c) and 3(c) for ^{208}Pb and ^{266}Pb , respectively. Let us discuss first the change of K_A with the mass number A , in the present case of isotopes. We see from the results for ^{208}Pb and ^{266}Pb that the finite nucleus compression modulus decreases when A increases. To understand this fact, it may be instructive to consider as a guideline the so-called leptodermous expansion of K_A [70]:

$$K_A = K_0 + K_{\text{surf}}A^{-1/3} + K_\tau I^2 + K_{\text{Coul}}Z^2A^{-4/3} + \dots \quad (24)$$

In this formula, K_0 is the compression modulus of symmetric infinite nuclear matter and K_{surf} , K_τ , and K_{Coul} correspond to the leading surface, volume-symmetry, and Coulomb

corrections that arise from the finite size, neutron-proton asymmetry, and electric charge of the nucleus.

In the scaling calculations carried out with mean field nuclear interactions, the coefficients K_{surf} , K_τ , and K_{Coul} are found to take negative values, and in particular K_τ may be large (especially in the relativistic mean field models) [6, 70, 71, 72, 73, 74]. In the case of the isotopic chain, the nuclear charge Z is fixed and therefore the neutron-proton asymmetry $I = (N - Z)/A$ increases when A increases. Then, although the surface and Coulomb contributions in Eq. (24) become a little less negative (because of the larger A value), the increase of the negative volume-symmetry contribution $K_\tau I^2$ dominates the variation of Eq. (24). The net result is that the value of K_A in isotopes decreases with a larger A . Needless to say, the terms considered in Eq. (24) do not account for K_A fully (there are for example surface-symmetry [$\mathcal{O}(I^2 A^{-1/3})$] and curvature [$\mathcal{O}(A^{-2/3})$] corrections, see e.g. Ref. [74]), but here we have concentrated on the leading contributions to be able to interpret the gross behavior of K_A . Let us recall in passing the nowadays well-known fact that one should not attempt to make a direct fit of Eq. (24) to experimental data on K_A to extract the individual values of the various coefficients, as these expansions in powers of $A^{-1/3}$ usually suffer from poor convergence [3, 6, 71, 72, 73, 74, 75].

We next discuss the dependence as a function of the coupling constant Λ_V of the scaling value of K_A (namely, K_A^{scal} given by Eq. (11) of Section II C). For both considered isotopes ^{208}Pb and ^{266}Pb , the compression modulus K_A^{scal} shows an upward trend with an increase of Λ_V , which is relatively more important in ^{266}Pb than in ^{208}Pb . The variation of K_A with Λ_V is due to the different density dependence of the symmetry energy when Λ_V changes, which modifies the value of K_τ and consequently K_A . The calculation of the values of the coefficients K_0 and K_{Coul} for a nuclear effective interaction involves only the properties of the EOS of symmetric nuclear matter [6, 71]. The isospin-dependent bulk term K_τ is given by the properties of the EOS of asymmetric nuclear matter [6, 71, 72, 73]. For the NL3 parameter sets with the Λ_V coupling that we are using in the present work we have $K_0 = 271.5$ MeV and $K_{\text{Coul}} = -6.45$ MeV, independently of Λ_V . We find the values -699 , -638 , -513 , and -381 MeV for the K_τ coefficient when we modify the Λ_V coupling from 0.00 to 0.03, respectively. This implies that the value of $K_0 + K_\tau I^2$ evolves from 240 MeV in NL3.00 to 255 MeV in NL3.03 for the ^{208}Pb nucleus, and that it undergoes an even larger variation from 169 MeV in NL3.00 to 216 MeV in NL3.03 for the ^{266}Pb isotope.

In scaling calculations with both relativistic and non-relativistic nuclear forces, the value of the surface incompressibility coefficient K_{surf} is found to approximately satisfy $K_{\text{surf}} \sim -K_0$ [6, 74]. On the other hand, the coefficient K_{Coul} does not vary much from one force to another. Therefore, the value of the isospin-dependent term K_τ of the nuclear incompressibility (not only the incompressibility K_0 of symmetric nuclear matter) has a basic role in the determination of the excitation energy of the GMR in the case of neutron-rich nuclei. Recent analyses of experimental data related to isospin diffusion in nuclear reactions [65, 76], the breathing mode of Sn isotopes [2], and neutron skins of nuclei [19] seem to favor, respectively, the constraints $K_\tau = -500 \pm 50$ MeV [65], $K_\tau = -550 \pm 100$ MeV [2] (or -500 ± 50 MeV following Ref. [72]), and $K_\tau = -500_{-100}^{+125}$ MeV [19], although there are large uncertainties in these extractions. We note that the celebrated Thomas-Fermi model of Myers and Świątecki [77, 78], which was fitted very precisely to the binding energies of a comprehensive set of 1654 nuclei, predicts an EOS that yields $K_\tau = -393$ MeV. All in all, the different available indications for the value of K_τ appear to fit in a range of about -650 MeV to -375 MeV. Incidentally, the range of K_τ values (-699 MeV to -381 MeV) that

we explore here with the NL3 model supplemented by the isoscalar-isovector Λ_V parameter is similar to this “empirical” range.

We have seen in Section II that the excitation energy of the GMR is determined by the ratio of the restoring force K_A to the mass parameter B_M of the monopole oscillation. As we have indicated, to replace the relativistic mass parameter B_M by its non-relativistic limit B_M^{nr} is a very good approximation. In practice, this implies that the value of B_M varies with the parameters of the nuclear interaction essentially in the same way as $\langle r^2 \rangle$ of the nucleus does [see Eq. (14)]. For a given nucleus, when the coupling constant Λ_V is increased, the rms radius of the matter distribution decreases because of the reduction of the neutron skin thickness originated by the non-linear isoscalar-isovector Λ_V interaction (we recall that the proton rms radius is to a good approximation independent of Λ_V). As a consequence, the value of the mass parameter of the GMR (analogously, the value of the m_1 sum rule (20) in the non-relativistic language) is reduced when the value of Λ_V increases.

Quantitatively, in passing from $\Lambda_V = 0.00$ to $\Lambda_V = 0.03$, the scaling value of K_A grows for ^{208}Pb (^{266}Pb) by approximately 2% (3.5%), whereas the mass parameter is reduced by 1.5% (4%). From this behavior of the restoring force and of the mass parameter, it is expected that the excitation energy of the GMR evaluated in the scaling approach will be enhanced in both lead isotopes ^{208}Pb and ^{266}Pb with increasing Λ_V values, i.e., with a softer density dependence of the symmetry energy of the model. This behavior is depicted in Figs. 2(d) and 3(d), where we can see that the enhancement of E_M^{scal} in a parameter set with a softer symmetry energy (i.e., a large Λ_V) is larger for a drip line nucleus like ^{266}Pb ($\sim 4\%$) than for a stable nucleus like ^{208}Pb ($\sim 2\%$). Though the changes are in principle small in magnitude, they are relatively sizable for such heavy systems.

Let us analyze now the results for the GMR in ^{208}Pb and ^{266}Pb that we have obtained through the constrained calculations described in Section II D. We first realize from Fig. 2 that K_A^{cons} and E_M^{cons} have in the case of the stable nucleus ^{208}Pb a similar behavior to the previously discussed scaling results when the density dependence of the symmetry energy is softened (i.e., with increasing values of the Λ_V coupling of the model or, analogously, with decreasing values of the neutron skin thickness of the nucleus because of the linear relationship between ΔR_{np} and Λ_V). For example, the increase of E_M^{cons} in ^{208}Pb from $\Lambda_V = 0.00$ to 0.03 is about 2%, as in the previous case of E_M^{scal} . According to Eq. (23) of Section II E, the separation between E_M^{cons} and E_M^{scal} is indicative of the width of the GMR resonance, and for ^{208}Pb this quantity is seen to be basically constant as a function of the Λ_V coupling. In contrast with the situation just described for ^{208}Pb , in the much more neutron-rich isotope ^{266}Pb the change of K_A^{cons} and E_M^{cons} with the softness of the symmetry energy exhibits a clearly different pattern from the results obtained in the scaling scheme. For ^{266}Pb , both quantities K_A^{cons} and E_M^{cons} not only do not increase with Λ_V , but they decrease significantly (K_A^{cons} by 30% and E_M^{cons} by 15% at $\Lambda_V = 0.03$).

To interpret the reduction of E_M^{cons} with the isoscalar-isovector Λ_V coupling in ^{266}Pb , it will be helpful to rewrite the expression $E_M^{\text{cons}} = (AK_A^{\text{cons}}/B_M)^{1/2}$ of Eq. (18) by approximating B_M with its non-relativistic form $B_M^{\text{nr}} = m A \langle r^2 \rangle$, and to write K_A^{cons} using the first expression given in Eq. (17). This results in

$$E_M^{\text{cons}} \simeq \sqrt{\frac{2A\langle r^2 \rangle/m}{-\frac{1}{2}A(\partial R_\eta^2/\partial \eta)_{\eta=0}}} \equiv \sqrt{\frac{\overline{m}_1}{\overline{m}_{-1}}}, \quad (25)$$

which in terms of the defined quantities \overline{m}_1 and \overline{m}_{-1} has virtually the same form that E_M^{cons} takes in the non-relativistic RPA formalism of sum rules [41, 42, 43]. We recall that, as in

Section IID, η denotes the constraining parameter and that $R_\eta^2 = \langle r^2 \rangle_\eta$.

We have already argued in Section IIIB that increasing the value of the Λ_V coupling reduces the value of $\langle r^2 \rangle$, and consequently of \overline{m}_1 , because of the associated reduction of the neutron radius of the nucleus at approximately constant proton radius. However, the decrease of $\langle r^2 \rangle$ in ^{266}Pb by 4% in going from $\Lambda_V = 0.00$ to 0.03 cannot explain the much more significant reduction of E_M^{cons} by 15% observed in Fig. 3(d). The point is that the denominator of Eq. (25) is very sensitive to the presence of loosely bound nucleons in the nucleus, as discussed in Ref. [44], which is precisely the situation that occurs in ^{266}Pb . When an isotope is close to the neutron drip line, the negative neutron chemical potential μ_n approaches zero, meaning that the system contains very weakly bound neutrons. These neutrons are very soft against compression and in the constrained calculations they give rise to a large increase of the absolute value of $(\partial R_\eta^2 / \partial \eta)_{\eta=0}$, i.e., of \overline{m}_{-1} in Eq. (25). This effect has been discussed for non-relativistic Skyrme forces in Ref. [44], where it can be related to the enhancement of the RPA strength in the low-energy region produced by the increase of the transitions to the continuum when the nucleus is close to the neutron drip line. In the present calculations, the increase of \overline{m}_{-1} near the neutron drip line is accentuated by the effect of the Λ_V coupling. Note that the parameter sets having smaller neutron skins (larger Λ_V) have also weaker binding energy of the last bound neutrons [23]. In our calculations for ^{266}Pb we find that the quantity \overline{m}_{-1} increases by 35% in passing from $\Lambda_V = 0$ to $\Lambda_V = 0.03$. Combined with the 4% decrease of \overline{m}_1 , this leads to the aforementioned reduction of the constrained excitation energy of the GMR in the ^{266}Pb nucleus between $\Lambda_V = 0$ and $\Lambda_V = 0.03$. The decreasing tendency of the constrained incompressibility K_A^{cons} with Λ_V in ^{266}Pb can be easily understood in similar terms to the case of E_M^{cons} if one takes into account Eq. (17) that relates K_A^{cons} with the inverse of the value of $(\partial R_\eta^2 / \partial \eta)_{\eta=0}$.

C. GMR along the Pb and Zr isotopic chains

In Ref. [44] we have investigated the behavior of the excitation energy and of the resonance width of the GMR in some isotopic chains in the non-relativistic Hartree-Fock framework by means of the sum rule approach [41, 42, 43] and Skyrme forces. We want now to explore the change of these properties of the GMR along the Pb and Zr isotopic chains as a function of the density dependence of the symmetry energy using the relativistic mean field model.

Because of the influence that the nuclear radii have on the energy of the GMR through the mass parameter [recall Eqs. (12)–(14) and (18)], we first display in Figs. 4(a) and 5(a) the evolution of the rms radii of the proton and neutron densities along the Pb and Zr isotopic chains. The results are shown as a function of the mass number A when one proceeds from the proton to the neutron drip line. We have obtained our results using two different values of the coupling constant Λ_V (0.00 and 0.03), corresponding to stiff and soft density dependences of the symmetry energy. Along each isotopic chain, the rms radii of the proton and neutron density distributions show an increasing tendency that roughly follows an $A^{1/3}$ law, until the neutron rms radius R_n deviates from this tendency when the drip line is approached. We see that in the whole span of both isotopic chains the rms radius R_p of the proton density almost does not vary with Λ_V . Or, in other words, the R_p observable is practically independent of the density dependence of the symmetry energy in this model. On the contrary, the rms radii of the neutron densities along a chain of isotopes are different for each value of the Λ_V coupling because R_n is very much sensitive to the density dependence of the symmetry energy.

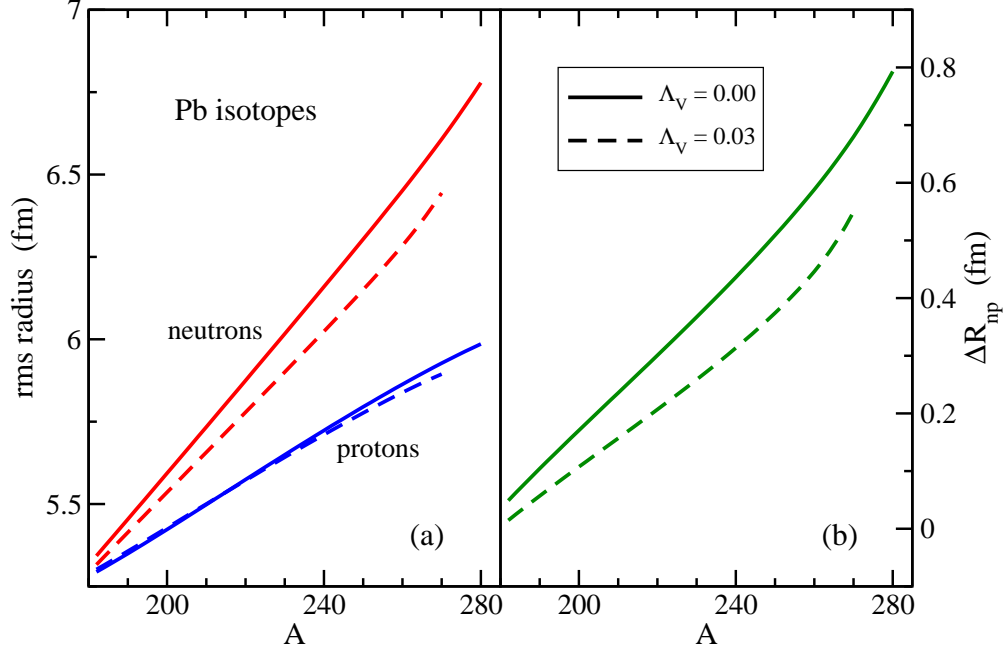


FIG. 4: (Color online) Neutron and proton rms radii (a) and neutron skin thickness (b) in the Pb isotopic chain for the NL3 model with $\Lambda_V = 0$ (stiff symmetry energy) and $\Lambda_V = 0.03$ (soft symmetry energy).

We can see in Figs. 4(a) and 5(a) that in an isotopic chain the neutron radii calculated with a parameter set with a soft density dependence of the symmetry energy ($\Lambda_V = 0.03$) are smaller and increase more slowly than when they are obtained with a parameter set where the symmetry energy is stiff. On the other hand, we also see that the neutron drip line is reached before (i.e., at smaller mass number A) if the model has a soft density dependence of the symmetry energy than when this dependence is stiff, which has been discussed earlier in Ref. [23]. Actually, we find in the numerical calculations that, for the same mass number, the neutron chemical potential μ_n is less negative in the soft case than in the stiff case, and consequently μ_n vanishes earlier. For example, in the present RETF calculations the neutron drip line (defined by $\mu_n = 0$) is reached at $A = 270$ and $A = 132$ for the Pb and Zr isotopes if $\Lambda_V = 0.03$, while these values are shifted by a few units to $A = 280$ and $A = 138$ if $\Lambda_V = 0.00$. Note that shell effects are absent in these semiclassical predictions of the drip lines. The proton drip lines are reached at $N \sim Z$ ($A = 182$ for Pb and $A = 78$ for Zr) owing to the Coulomb barrier. Thus, because one deals with almost symmetric matter in the proton-rich side of the isotopic chains, the position of the proton drip line is practically unaffected by the symmetry energy and its dependence on the nuclear density.

The variation of the neutron skin thickness $\Delta R_{np} = R_n - R_p$ of the Pb and Zr isotopes with the isoscalar-isovector Λ_V interaction is shown in Figs. 4(b) and 5(b). Due to its definition, the neutron skin thickness changes in accordance with the commented tendencies of the neutron and proton rms radii. It increases with mass number A within an isotopic chain, and it is larger for parameter sets whose symmetry energy is stiffer.

We depict in Fig. 6 the average excitation energies of the GMR evaluated with the scaling and constrained calculations for the chain of Pb isotopes. We have used the values 0.00 and 0.03 for the non-linear ω - ρ interaction Λ_V . For the same reasons pointed out in our previous

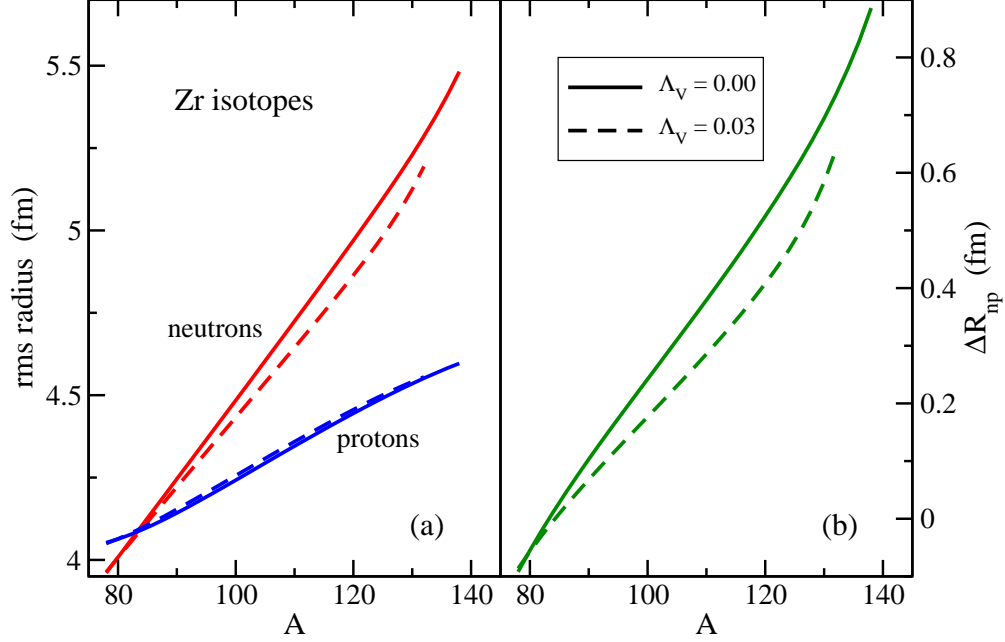


FIG. 5: (Color online) Neutron and proton rms radii (a) and neutron skin thickness (b) in the Zr isotopic chain for the NL3 model with $\Lambda_V = 0$ (stiff symmetry energy) and $\Lambda_V = 0.03$ (soft symmetry energy).

discussion about the ^{208}Pb and ^{266}Pb isotopes, the scaled and constrained estimates of the excitation energy of the GMR show a downward tendency with increasing mass number A when one proceeds along the Pb isotopic chain, which is more noticeable for E_M^{cons} than for E_M^{scal} . As a function of the Λ_V parameter, the scaling energies E_M^{scal} calculated using a parameter set with a symmetry energy that has a soft density dependence are systematically larger than if this dependence is stiff. Similarly to our discussion of the scaling results for ^{208}Pb and ^{266}Pb , this behavior of E_M^{scal} with Λ_V is a direct consequence of the variation of the values of the total rms radius and of the values of the scaling finite nucleus compression modulus (the former are smaller, and the latter are larger, for a parameter set with $\Lambda_V = 0.03$ than for a parameter set with $\Lambda_V = 0.00$).

At variance with the uniformity displayed by the E_M^{scal} results, the constrained estimate E_M^{cons} of the excitation energy of the GMR has a distinct feature with Λ_V below and above $A \simeq 254$. If the mass number is below $A \simeq 254$, E_M^{cons} is larger when the parameter set has a soft density dependence of the symmetry energy ($\Lambda_V = 0.03$) than when the density dependence is stiff ($\Lambda_V = 0.00$). However, this tendency is reversed starting from $A \simeq 254$ to the neutron drip line when the isotopes are more exotic. The situation can be explained as follows. The effect of the Λ_V parameter in a given nucleus is to reduce its rms neutron radius R_n , with almost the same R_p , which means that the system becomes on average more compact. As long as the nucleus does not be extremely neutron rich, if it is more compact, the effect of the constraining parameter η on the nuclear rms radius is less, and therefore the absolute value of $(\partial R_\eta^2 / \partial \eta)_{\eta=0}$ in the denominator of Eq. (25) for E_M^{cons} is smaller. This explains the larger magnitude of the constrained excitation energy of the GMR at $\Lambda_V = 0.03$, compared to the case of $\Lambda_V = 0.00$, in the Pb isotopes lighter than $A \simeq 254$. On the other hand, a point is reached in mass number ($A \simeq 254$ in the present context) where the isotopes are so neutron rich, and so close to the neutron drip line, that the last neutrons become

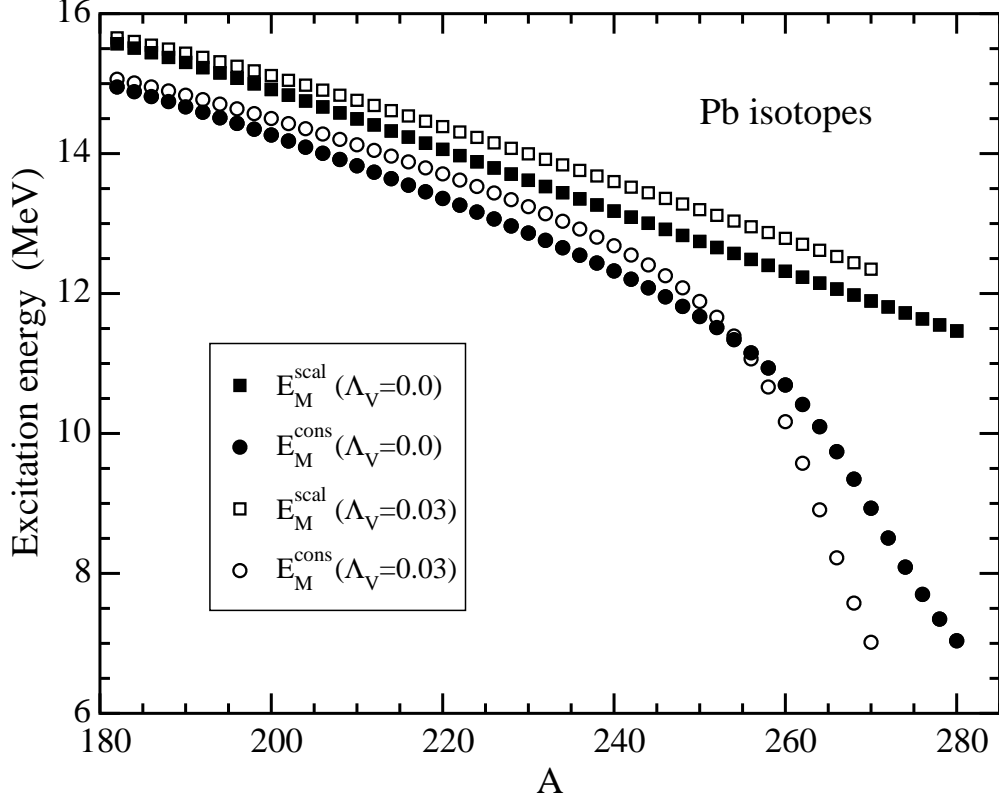


FIG. 6: Mass-number dependence of the excitation energy of the giant monopole resonance in the Pb isotopic chain for the NL3 model with $\Lambda_V = 0$ (stiff symmetry energy) and $\Lambda_V = 0.03$ (soft symmetry energy), in the scaling and constrained approaches.

very weakly bound. These outer neutrons are very soft against compression. As a result of their specific contribution to R_η^2 when one applies an external constraint, the absolute value of $(\partial R_\eta^2 / \partial \eta)_{\eta=0}$ increases sharply instead of decreasing. This originates the large reduction of E_M^{cons} seen in Fig. 6 close to the neutron drip line. A comparable sharp decrease of the excitation energy of the GMR, however, is not present in the scaling calculations because the discussed effect does not arise in a self-similar scaling of the density of the nucleus. The reduction of E_M^{cons} near the neutron drip line is even larger in the calculation with the softer symmetry energy than in the calculation with the stiffer symmetry energy, by the same effect discussed previously for the ^{266}Pb nucleus in Section III B (namely, the outer neutrons are more weakly bound in the models with a soft symmetry energy).

We may take $\sigma = \frac{1}{2}[(E_M^{\text{scal}})^2 - (E_M^{\text{cons}})^2]^{1/2}$ as an estimate of the width of the GMR, in analogy with the non-relativistic framework [41, 42, 43] (see Section II E). From the separation observed in Fig. 6 between the values of the E_M^{scal} and E_M^{cons} energies, at either $\Lambda_V = 0.00$ or $\Lambda_V = 0.03$, one expects that the width of the resonance will be largely independent of the mass number and of the density dependence of the symmetry energy for all of the Pb nuclei located in the region between the proton-rich side of the isotopic chain till $A \simeq 230$ –240. However, E_M^{cons} starts to depart from E_M^{scal} pronouncedly after $A \simeq 240$ and, as a consequence, the resonance width should display a sharp increase for the Pb isotopes reaching the neutron drip line. We see from Fig. 6 that this effect is predicted to be stronger when the nuclear interaction has a symmetry energy with a soft density dependence than

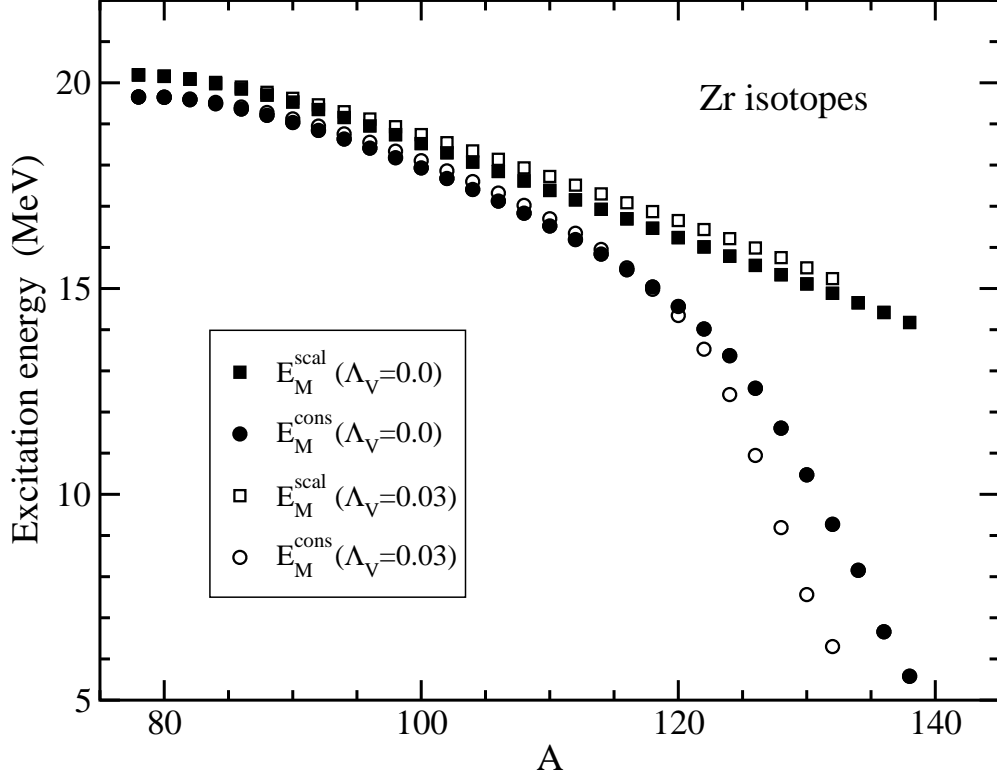


FIG. 7: Mass-number dependence of the excitation energy of the giant monopole resonance in the Zr isotopic chain for the NL3 model with $\Lambda_V = 0$ (stiff symmetry energy) and $\Lambda_V = 0.03$ (soft symmetry energy), in the scaling and constrained approaches.

when the density dependence is stiff. As discussed in, e.g., Ref. [44] in the context of non-relativistic calculations with Skyrme forces, the value of the estimate σ of the GMR width provides a qualitative idea about the distribution of the RPA strength. A small width σ indicates that the RPA strength of the GMR is basically concentrated in a narrow single peak, whereas a large width σ suggests that the peak is broad, or even that the RPA strength may be fragmented into several peaks. The large value of $\overline{m}_{-1} \propto -(\partial R_\eta^2 / \partial \eta)_{\eta=0}$ [see Eq. (25)] that one finds in the constrained calculations for the Pb nuclei close to the neutron drip line, points towards an enhancement of the RPA strength in the low-energy region in these exotic nuclei, due to transitions from the last weakly bound single-particle levels to the continuum [44]. This effect, which has a quantal origin, is, however, accounted at least on average by the semiclassical calculations [44].

Lastly, we present in Fig. 7 our calculated results for the excitation energies of the GMR in the Zr isotopic chain. The variation of the excitation energies obtained in the scaling scheme as a function of the mass number A and of the Λ_V coupling is qualitatively similar to the pattern exhibited by the Pb isotopes. That is, the excitation energies E_M^{scal} show a monotonic decrease with increasing mass number, and they are larger when calculated with parameter sets having a soft density dependence of the symmetry energy than when this dependence is stiff. However, the differences between the values of $E_M^{\text{scal}}(\Lambda_V = 0.00)$ and $E_M^{\text{scal}}(\Lambda_V = 0.03)$ are smaller compared to the chain of the Pb isotopes because of the smaller isospin content of the Zr isotopes. Concerning the results for the constrained excitation energies in Zr, the value of E_M^{cons} shows a stronger dependence on the mass number

in approaching the neutron drip line than the scaling estimate. The excitation energy E_M^{cons} for zirconium is to a large extent independent of the Λ_V coupling as long as $A \lesssim 120$. But afterwards, when the heavier isotopes of the Zr chain approach the neutron drip line, the value of $E_M^{\text{cons}}(\Lambda_V = 0.03)$ becomes visibly lower than the value of $E_M^{\text{cons}}(\Lambda_V = 0.00)$, as it also happened in the most neutron-rich isotopes of the Pb chain.

In consonance with the behavior of E_M^{scal} and E_M^{cons} found in Fig. 7, the resonance width σ predicted for the Zr nuclei would remain practically constant till $A \simeq 100$. Then, the width σ would start increasing moderately between $A \simeq 100$ and $A \simeq 120$, because of the slight gradual separation between E_M^{scal} and E_M^{cons} in these isotopes. Finally, the resonance width would be dramatically enhanced in the region of the most neutron-rich Zr isotopes, where the effect is largely reinforced by having a soft symmetry energy in the nuclear interaction.

IV. SUMMARY AND CONCLUSIONS

In this paper we have analyzed the influence of the density dependence of the symmetry energy on the excitation energy of the isoscalar giant monopole resonance. Although this energy is mainly ruled by the compression modulus of the symmetric nuclear matter, the symmetry energy also plays a role in the value of this excitation energy in neutron-rich nuclei.

In order to do this study we have used the relativistic mean field model supplemented by an additional ω - ρ interaction which, as a function of the corresponding coupling constant Λ_V , allows to generate different parameter sets that basically differ among them in the density dependence of the symmetry energy only. For moderate values of the coupling constant Λ_V , this relativistic mean field model predicts in finite nuclei almost the same binding energy and proton rms radius whereas the neutron rms radius decreases almost linearly with increasing values of the coupling constant Λ_V .

The excitation energy of the isoscalar giant monopole resonance is estimated using the semiclassical relativistic extended Thomas-Fermi theory. This approximation allows to obtain the energy of the breathing mode in two different ways using the scaling model and performing constrained calculations. These semiclassical calculations nicely reproduce the average energies E_3 and E_1 obtained from the more fundamental relativistic RPA calculations.

In order to study the dependence of the excitation energy of the isoscalar giant monopole resonance on the neutron-proton asymmetry, we have calculated the semiclassical energy estimates E_M^{scal} (scaled) and E_M^{cons} (constrained) along the isotopic chains of Pb and Zr from the proton to the neutron drip lines. We can also obtain some information about the distribution of the RPA strength from the resonance width computed using these two estimates of the excitation energy.

As is known, the excitation energy of the breathing mode decreases with increasing mass number, at least for stable nuclei. The semiclassical relativistic estimates of the excitation energy show the same behaviour in approaching the neutron drip line, as it happens in the non-relativistic frame. In the scaling model the restoring force and the mass denominator grow when the mass number increases. However, the enhancement of the restoring force is smaller than the one of the mass denominator, which explains the global downwards tendency of the scaled excitation energy of the giant monopole resonance when the mass number moves towards the neutron drip line along an isotopic chain. The average excitation energies computed semiclassically performing constrained calculations follow, in general, a similar

behaviour to the one exhibit by the the scaled energies. However, the decreasing tendency is more pronounced in the case of constrained calculations. In this case the constrained finite nucleus compressibility decreases noticeably near the neutron drip line and, consequently, the nucleus becomes very soft against compression. This fact simulates the enhancement of the RPA strength in the low energy region due to transitions to the continuum from the weakly bound single-particle levels in very neutron-rich nuclei.

The excitation energy of the isoscalar giant monopole resonance in nuclei with a moderate or large neutron-proton asymmetries also depends, to certain extent, on the density content of the symmetry energy. Along the whole Pb and Zr isotopic chains the scaled estimate of the excitation energy is larger for parameter sets that have a symmetry energy with a soft density dependence than if this dependence is stiff. However, this trend is different if the estimate of the excitation energy is obtained through a constrained calculation. For nuclei with a relatively moderate neutron excess, the behaviour of this estimate as a function of the density dependence of the symmetry energy is similar to the one exhibited by the scaled excitation energy. However, this tendency is reversed in nuclei near the neutron drip line where the constrained excitation energy decreases when Λ_V increases. In this case the outer neutrons of the very neutron-rich nuclei are so soft that the constrained finite nucleus compression modulus is strongly reduced decreasing, consequently, the constrained estimate of the excitation energy of the giant monopole resonance.

In our study we have considered values of the coupling constant Λ_V in the range between 0.00 and 0.03. In this range of Λ_V the rms radius of the neutron density of the nucleus ^{208}Pb changes roughly by a 1 % which simulates the expected experimental error of its measurement in the future PREX experiment. Thus the variation with Λ_V of the different magnitudes considered in this work, and in particular of the excitation energies of the giant monopole resonances, shall be understood as an estimate of their theoretical uncertainty if the slope of the symmetry energy at $\rho=0.10\text{ fm}^{-3}$ lies in the range of values correlated with the ones of the neutron skin provided by the PREX experiment.

Acknowledgments

M.C., X.R., and X.V. would like to thank J. Piekarewicz for useful conversations. They acknowledge support from the Consolider Ingenio 2010 Programme CPAN CSD2007-00042 and grants FIS2008-01661 from MEC and FEDER, and 2005SGR-00343 from Generalitat de Catalunya. X.R. also acknowledges grant AP2005-4751 from MEC. S.K.P. and B.K.S. acknowledge the support of CSIR (No. 03(1060) 06/EMR-II), Government of India. P.D.S. acknowledges support from the UK Science and Technology Facilities council under grants PP/F000596/1 and ST/F012012/1.

APPENDIX A: EQUATIONS OF THE RELATIVISTIC EXTENDED THOMAS-FERMI MODEL

We have introduced the energy density of the relativistic nuclear mean field model supplemented by an isoscalar-isovector mixed ω - ρ interaction in Eq. (1) of the text. Following Refs. [49, 50, 51, 52, 53], in the relativistic extended Thomas-Fermi approach the expression

of the nucleonic part \mathcal{E} is written as $\mathcal{E} = \mathcal{E}_0 + \mathcal{E}_2$, where

$$\mathcal{E}_0 = \sum_{q=n,p} \frac{1}{8\pi^2} \left[k_{Fq} \epsilon_{Fq}^3 + k_{Fq}^3 \epsilon_{Fq} - m^{*4} \ln \frac{k_{Fq} + \epsilon_{Fq}}{m^*} \right] \quad (\text{A1})$$

and

$$\mathcal{E}_2 = \sum_{q=n,p} \left[C_{1q}(k_{Fq}, m^*) (\nabla \rho_q)^2 + C_{2q}(k_{Fq}, m^*) (\nabla \rho_q \cdot \nabla m^*) + C_{3q}(k_{Fq}, m^*) (\nabla m^*)^2 \right]. \quad (\text{A2})$$

The leading term \mathcal{E}_0 is the contribution of the pure Thomas-Fermi part, whereas the term \mathcal{E}_2 contains the gradient corrections of order \hbar^2 . The variables k_{Fq} , m^* , and ϵ_{Fq} are, respectively, the local Fermi momentum $k_{Fq} = (3\pi^2 \rho_q)^{1/3}$, the Dirac effective mass $m^* = m - \Phi$, and the dispersion relation $\epsilon_{Fq} = (k_{Fq}^2 + m^{*2})^{1/2}$ of the effective particle, with $q = n$ for neutrons and $q = p$ for protons. The coefficients C_{iq} stand for the following analytic functions of k_{Fq} and $m^* = m - \Phi$:

$$\begin{aligned} C_{1q} &= \frac{\pi^2}{24 k_{Fq}^3 \epsilon_{Fq}^2} \left(\epsilon_{Fq} + 2k_{Fq} \ln \frac{k_{Fq} + \epsilon_{Fq}}{m^*} \right), \\ C_{2q} &= \frac{m^*}{6 k_{Fq} \epsilon_{Fq}^2} \ln \frac{k_{Fq} + \epsilon_{Fq}}{m^*}, \\ C_{3q} &= \frac{k_{Fq}^2}{24 \pi^2 \epsilon_{Fq}^2} \left[\frac{\epsilon_{Fq}}{k_{Fq}} - \left(2 + \frac{\epsilon_{Fq}^2}{k_{Fq}^2} \right) \ln \frac{k_{Fq} + \epsilon_{Fq}}{m^*} \right]. \end{aligned} \quad (\text{A3})$$

The RETF ground-state densities and meson fields are calculated by solving by numerical iteration the Euler-Lagrange equations associated to the energy density (1), with the constraint of baryon number conservation (which is imposed through Lagrange multipliers μ_q , the chemical potentials of neutrons and protons):

$$\begin{aligned} &\epsilon_{Fq} + W + \frac{1}{2} [\mathcal{A} + (\mathcal{A} + B) \tau_{3q}] \\ &- 2C_{1q} \Delta \rho_q - C_{2q} \Delta m^* - \frac{\partial C_{1q}}{\partial \rho_q} (\nabla \rho_q)^2 - 2 \frac{\partial C_{1q}}{\partial m^*} (\nabla \rho_q \cdot \nabla m^*) \\ &- \left(\frac{\partial C_{2q}}{\partial m^*} - \frac{\partial C_{3q}}{\partial \rho_q} \right) (\nabla m^*)^2 = m + \mu_q, \end{aligned} \quad (\text{A4})$$

$$(\Delta - m_s^2) \Phi = -g_s^2 \left(\rho_s - \frac{\kappa}{2!} \Phi^2 - \frac{\lambda}{3!} \Phi^3 \right) \equiv -g_s^2 \rho_s^{\text{eff}}, \quad (\text{A5})$$

$$(\Delta - m_v^2) W = -g_v^2 (\rho - 2\Lambda_V B^2 W), \quad (\text{A6})$$

$$(\Delta - m_\rho^2) B = -g_\rho^2 (\rho_3 - 2\Lambda_V B W^2), \quad (\text{A7})$$

$$\Delta \mathcal{A} = -\rho_p. \quad (\text{A8})$$

We have $\tau_{3q} = +1$ for protons and $\tau_{3q} = -1$ for neutrons. The baryon density is $\rho = \rho_p + \rho_n$, whereas $\rho_3 = \frac{1}{2}(\rho_p - \rho_n)$ is the isovector density of the nucleus. Finally, the RETF expression of the scalar density ρ_s entering Eq. (A5) is given by

$$\begin{aligned}
\rho_s &= \frac{\delta \mathcal{E}}{\delta m^*} = \frac{\delta \mathcal{E}_0}{\delta m^*} + \frac{\delta \mathcal{E}_2}{\delta m^*} = \rho_{s0} + \rho_{s2} \\
&= \sum_q \frac{m^*}{2\pi^2} \left[k_{Fq} \epsilon_{Fq} - m^{*2} \ln \frac{k_{Fq} + \epsilon_{Fq}}{m^*} \right] \\
&\quad - \sum_q \left[C_{2q} \Delta \rho_q + 2C_{3q} \Delta m^* + \left(\frac{\partial C_{2q}}{\partial \rho_q} - \frac{\partial C_{1q}}{\partial m^*} \right) (\nabla \rho_q)^2 \right. \\
&\quad \left. + 2 \frac{\partial C_{3q}}{\partial \rho_q} (\nabla \rho_q \cdot \nabla m^*) + \frac{\partial C_{3q}}{\partial m^*} (\nabla m^*)^2 \right]. \tag{A9}
\end{aligned}$$

APPENDIX B: KLEIN-GORDON EQUATIONS OF THE SCALED MESON FIELDS

In this Appendix we illustrate some aspects of the calculation of the derivatives of the scaled meson fields upon the scaling parameter α that we have used to represent the collective coordinate of the monopole oscillation of the nucleus. In view of Eq. (4) for the scaled baryon density ρ_α , i.e., $\rho_\alpha(\mathbf{r}) = \alpha^3 \rho(\alpha \mathbf{r})$, and of the field equation (A6) obeyed by the omega-meson field W , the scaled field W_α fulfils the Klein-Gordon equation

$$(\Delta_{\mathbf{u}} - m_v^2/\alpha^2) W_\alpha(\mathbf{u}) = -g_v^2 \left(\alpha \rho(\mathbf{u}) - \frac{2\Lambda_V}{\alpha^2} B_\alpha(\mathbf{u})^2 W_\alpha(\mathbf{u}) \right), \tag{B1}$$

where we have introduced the coordinate $\mathbf{u} \equiv \alpha \mathbf{r}$. On differentiating Eq. (B1) with respect to the scaling parameter α we have

$$\begin{aligned}
&\left(\Delta_{\mathbf{u}} - \frac{m_v^2}{\alpha^2} \right) \frac{\partial W_\alpha}{\partial \alpha} = \\
&-g_v^2 \left(\rho - \frac{2m_v^2}{g_v^2} \frac{W_\alpha}{\alpha^3} + \frac{4\Lambda_V}{\alpha^3} B_\alpha^2 W_\alpha - \frac{4\Lambda_V}{\alpha^2} B_\alpha W_\alpha \frac{\partial B_\alpha}{\partial \alpha} - \frac{2\Lambda_V}{\alpha^2} B_\alpha^2 \frac{\partial W_\alpha}{\partial \alpha} \right). \tag{B2}
\end{aligned}$$

If we now set $\alpha = 1$, the solution of this equation allows us to obtain the value of the derivative $\partial W_\alpha / \partial \alpha|_{\alpha=1}$. On the other hand, let us multiply Eq. (B1) by $\partial W_\alpha / \partial \alpha$ and Eq. (B2) by W_α and subtract the two resulting equations. Then, integrating the result over the whole space and using Green's identity, it is easy to obtain the relationship

$$\int d\mathbf{u} \left[\frac{1}{2} \rho \frac{\partial W_\alpha}{\partial \alpha} + \frac{2\Lambda_V}{\alpha^3} B_\alpha W_\alpha^2 \frac{\partial B_\alpha}{\partial \alpha} \right] = \int d\mathbf{u} \left[\frac{1}{2\alpha} \rho W_\alpha + \frac{2\Lambda_V}{\alpha^4} B_\alpha^2 W_\alpha^2 - \frac{m_v^2}{g_v^2} \frac{W_\alpha^2}{\alpha^4} \right], \tag{B3}$$

where the expression on the r.h.s. has the advantage that it does not contain derivatives of the fields with respect to the parameter α . One can work out the equivalent equations for the scaled isovector ρ -meson field in the same way we have shown here for the W field.

In practice, one simply has to replace $(W_\alpha, B_\alpha, \rho, m_v, g_v)$ by $(B_\alpha, W_\alpha, \rho_3, m_\rho, g_\rho)$ in Eqs. (B1)–(B3).

In the case of the equations for the scalar field one has to take account of the terms that arise due to the fact that the scalar density ρ_s is itself a function of the scalar field. Following the same steps as above, from the Klein-Gordon equation

$$(\Delta_{\mathbf{u}} - m_s^2/\alpha^2)\Phi_\alpha(\mathbf{u}) = -\alpha g_s^2 \tilde{\rho}_s^{\text{eff}}(\mathbf{u}) \quad (\text{B4})$$

for the scaled scalar field Φ_α , one readily arrives at the equation

$$\left(\Delta_{\mathbf{u}} - \frac{m_s^2}{\alpha^2}\right) \frac{\partial \Phi_\alpha}{\partial \alpha} = -g_s^2 \left(\tilde{\rho}_s^{\text{eff}} - \alpha \frac{\partial \tilde{\rho}_s^{\text{eff}}}{\partial \alpha} - \frac{2m_s^2}{g_s^2} \frac{\Phi_\alpha}{\alpha^3} \right), \quad (\text{B5})$$

whose solution at $\alpha = 1$ provides the value of $\partial \Phi_\alpha / \partial \alpha|_{\alpha=1}$. By a similar procedure to that followed for the W field, one can derive the relationship

$$\int d\mathbf{u} \left[-\frac{1}{2} \tilde{\rho}_s^{\text{eff}} \frac{\partial \Phi_\alpha}{\partial \alpha} + \frac{1}{2} \Phi_\alpha \frac{\partial \tilde{\rho}_s^{\text{eff}}}{\partial \alpha} \right] = \int d\mathbf{u} \left[-\frac{1}{2\alpha} \tilde{\rho}_s^{\text{eff}} \Phi_\alpha - \frac{m_s^2}{g_s^2} \frac{\Phi_\alpha^2}{\alpha^4} \right]. \quad (\text{B6})$$

We have used the results (B3) and (B6) in Section II B of the text to obtain Eq. (8) for the first derivative with respect to α of the scaled energy of the RMF model plus a mixed ω - ρ interaction.

-
- [1] D. H. Youngblood, H. L. Clark, and Y.-W. Lui, Phys. Rev. Lett. **82**, 691 (1999).
 - [2] T. Li et al, Phys. Rev. Lett. **99**, 162503 (2007).
 - [3] J. P. Blaizot, J. F. Berger, J. Dechargé, and M. Girod, Nucl. Phys. **A591**, 435 (1995).
 - [4] M. Farine, J. M. Pearson, and F. Tondeur, Nucl. Phys. **A615**, 135 (1997).
 - [5] I. Hamamoto, H. Sagawa, and X. Z. Zhang, Phys. Rev. C **56**, 3121 (1997).
 - [6] G. Colò, N. Van Giai, J. Meyer, K. Bennaceur, and P. Bonche, Phys. Rev. C **70**, 024307 (2004).
 - [7] Zhong-yu Ma, N. Van Giai, A. Wandelt, D. Vretenar, and P. Ring, Nucl. Phys. **A686**, 173 (2001).
 - [8] B. G. Todd-Rutel and J. Piekarewicz, Phys. Rev. Lett. **95**, 122501 (2005).
 - [9] J. M. Lattimer and M. Prakash, Science **304**, 536 (2004); Phys. Rep. **442**, 109 (2007).
 - [10] T. Klähn et al., Phys. Rev. C **74**, 035802 (2006).
 - [11] J. Piekarewicz, Phys. Rev. C **76**, 064310 (2007).
 - [12] J. Xu, L. W. Chen, B. A. Li, and H. R. Ma, arXiv:0901.2309
 - [13] I. Bednarek and R. Manka, arXiv:0905.0131.
 - [14] B. A. Brown, Phys. Rev. Lett. **85**, 5296 (2000).
 - [15] C. J. Horowitz and J. Piekarewicz. Phys. Rev. Lett. **86**, 5647 (2001).
 - [16] C. J. Horowitz and J. Piekarewicz. Phys. Rev. C **64**, 062802(R) (2001).
 - [17] C. J. Horowitz and J. Piekarewicz. Phys. Rev. C **66**, 055803 (2002).
 - [18] P. Danielewicz, Nucl. Phys. **A727**, 233 (2003).
 - [19] M. Centelles, X. Roca-Maza, X. Viñas, and M. Warda, Phys. Rev. Lett. **102**, 122502 (2009).
 - [20] S. Typel and B. A. Brown, Phys. Rev. C **64**, 027302 (2001).
 - [21] M. Centelles, M. Del Estal, X. Viñas, and S. K. Patra, in *The Nuclear Many-Body Problem 2001*, Vol. 53 of NATO Advanced Studies Institute Series B: Physics, edited by W. Nazarewicz and D. Vretenar (Kluwer, Dordrecht, 2002), p. 97.
 - [22] M. Baldo, C. Maieron, P. Schuck and X. Viñas, Nucl. Phys. **A591** 435 (1995).
 - [23] B. G. Todd and J. Piekarewicz, Phys. Rev. C **67**, 044317 (2003).
 - [24] Tapas Sil, M. Centelles, X. Viñas, and J. Piekarewicz, Phys. Rev. C **71**, 045502 (2005).
 - [25] I. Angeli, At. Data Nucl. Data Tables **87**, 185 (2004).
 - [26] G. A. Lalazissis, J. König, and P. Ring, Phys. Rev. C **55**, 540 (1997).
 - [27] K. Kumar, P. A. Souder, R. Michaels, and G. M. Urciuoli, spokespersons, <http://hallaweb.jlab.org/parity/prex>.
 - [28] Dao T. Khoa, W. von Oertzen, and A. A. Ogloblin, Nucl. Phys. **A602**, 98 (1996).
 - [29] A. Ozawa, T. Suzuki and I. Tanihata, Nucl. Phys. **A693** 32 (2001).
 - [30] Dao T. Khoa, H. S. Than, T. H. Nam, M. Grasso, and N. Van Giai, Phys. Rev. C **69**, 044605 (2004).
 - [31] D. Seweryniak and T. L. Khoo (eds.), *Nuclei at the Limits*, Argonne, USA, 26-30 July 2004, AIP Conference Proceedings, Vol. 764 (Springer, 2005).
 - [32] *Proceedings of the Conference ENAM'04 on Exotic Nuclei and Atomic Masses*, Pine Mountain, USA, 12-16 September 2004, edited by C. J. Gross, W. Nazarewicz, and K. P. Rykaczewski, Eur. Phys. J. A **25**, s01 (2005); *Proceedings of the Conference ENAM'08 on Exotic Nuclei and Atomic Masses*, Ryn, Poland, 7-13 September 2008, to be published in Eur. Phys. J. A.
 - [33] B. D. Serot and J. D. Walecka, Adv. Nucl. Phys. **16**, 1 (1986).

- [34] I. Hamamoto, H. Sagawa, and X. Z. Zhang, Phys. Rev. C **55**, 2361 (1997); J. Phys. **G** **24**, 1417 (1998); Nucl. Phys. **A648**, 203 (1999).
- [35] M. N. Harakeh and A. van der Woude, *Giant Resonances* (Oxford University Press, New York, 2001).
- [36] J. Piekarewicz, Phys. Rev. C **66**, 034305 (2002).
- [37] D. Vretenar, T. Nikšić, and P. Ring, Phys. Rev. C **68**, 024310 (2003).
- [38] B. K. Agrawal, S. Shlomo, and V. K. Au, Phys. Rev. C **68**, 031304(R) (2003).
- [39] J. Piekarewicz, Phys. Rev. C **69**, 041301(R) (2004).
- [40] J. Piekarewicz, Phys. Rev. C **76**, 031301(R) (2007).
- [41] O. Bohigas, A. Lane, and J. Martorell, Phys. Rep. **51**, 267 (1979).
- [42] E. Lipparini and S. Stringari, Phys. Rep. **175**, 103 (1989).
- [43] P. Gleissl, M. Brack, J. Meyer, and P. Quentin, Ann. Phys. (NY) **197**, 205 (1990).
- [44] M. Centelles, X. Viñas, S. K. Patra, J. N. De, and Tapas Sil, Phys. Rev. C **72** 014304 (2005).
- [45] Tapas Sil, S. Shlomo, B. K. Agrawal, and P.-G. Reinhard, Phys. Rev. C **73**, 034316 (2006).
- [46] L. Capelli, G. Colò, and J. Li, Phys. Rev. C **79**, 054329 (2009).
- [47] M. Centelles, M. Pi, X. Vinas, F. Garcias, and M. Barranco, Nucl. Phys. **A510**, 397 (1990).
- [48] Li Guo-Qiang, J. Phys. **G17**, 1 (1991).
- [49] M. Centelles, X. Viñas, M. Barranco and P. Schuck, Ann. Phys. (NY) **221**, 165 (1993).
- [50] M. Centelles, X. Viñas, M. Barranco, S. Marcos and R.J. Lombard, Nucl. Phys. **A537** 486 (1992).
- [51] C. Speicher, E. Engel and R.M. Dreizler, Nucl. Phys. **A562** 569 (1993).
- [52] M. Centelles and X. Viñas, Nucl. Phys. **A563** 173 (1993).
- [53] M. Centelles, M. Del Estal and X. Viñas, Nucl. Phys. **A635** 193 (1998).
- [54] S.K. Patra, X. Viñas, M. Centelles and M. Del Estal, Phys. Lett. **B523** 67 (2001).
- [55] S.K. Patra, X. Viñas, M. Centelles and M. Del Estal, Nucl. Phys. **A703** 240 (2002).
- [56] S. Nishizaki, H. Kurasawa, and T. Suzuki, Nucl. Phys. **A462** 689 (1987).
- [57] Chaoyuan Zhu and Xi-Jun Qiu, J. Phys. **G17** L11 (1991).
- [58] T. Maruyama and T. Suzuki, Phys. Lett. **B219** 43 (1989).
- [59] H.F. Boersma, R. Malfliet and O. Scholten, Phys. Lett. **B269** 1 (1991).
- [60] M.V. Stoitsov, P. Ring and M.M. Sharma, Phys. Rev. C **50** 1445 (1994).
- [61] M.V. Stoitsov, M.L. Cescato, P. Ring and M.M. Sharma, J. Phys. **G20**, L149 (1994).
- [62] A. W. Steiner, M. Prakash, J. M. Lattimer, and P. J. Ellis, Phys. Rep. **411**, 325 (2005).
- [63] V. Baran, M. Colonna, V. Greco, and M. Di Toro, Phys. Rep. **410**, 335 (2005).
- [64] D. V. Shetty, S. J. Yennello, and G. A. Souliotis, Phys. Rev. C **76**, 024606 (2007).
- [65] B. A. Li, L. W. Chen, and C. M. Ko, Phys. Rep. **464**, 113 (2008).
- [66] M. B. Tsang, Y. Zhang, P. Danielewicz, M. Famiano, Z. Li, W. G. Lynch, and A. W. Steiner, Phys. Rev. Lett. **102**, 122701 (2009).
- [67] A. Klimkiewicz et al, Phys. Rev. C **76**, 051603(R) (2007).
- [68] L. Trippa, G. Colò, and E. Vigezzi, Phys. Rev. C **77**, 061304(R) (2008).
- [69] P. Roy Chowdhury, D. N. Basu, and C. Samanta, arXiv:0905.1599.
- [70] J. P. Blaizot, Phys. Rep. **64** 171 (1980).
- [71] T. v. Chossy and W. Stocker, Phys. Rev. C **56**, 2518 (1997).
- [72] H. Sagawa, S. Yoshida, G. M. Zeng, J. Z. Gu, and X. Z. Zhang, Phys. Rev. C **76**, 034327 (2007).
- [73] J. Piekarewicz and M. Centelles, Phys. Rev. C **79**, 054311 (2009).
- [74] S. K. Patra, M. Centelles, X. Viñas, and M. Del Estal, Phys. Rev. C **65**, 044304 (2002).

- [75] W. D. Myers and W. J. Świątecki, Nucl. Phys. **A587**, 92 (1995).
- [76] L. W. Chen, C. M. Ko, and B. A. Li, Phys. Rev. Lett. **94**, 032701 (2005).
- [77] W. D. Myers and W. J. Świątecki, Nucl. Phys. **A601**, 141 (1996).
- [78] W. D. Myers and W. J. Świątecki, Phys. Rev. C **57**, 3020 (1998).